

MICROCOPY RESOLUTION TEST CHART
NATIONAL BUREAU OF STANDARDS-1963-A

AD-A163 961



An Experimental Study of Clustered Nozzles
with Variable Shrouds

THESIS

James R. Moran
Captain, US Army

AFIT/GAE/AA/85D-11

DISTRIBUTION STATEMENT A
Approved for public release
Distribution Unlimited

DTIC
ELECTE
FEB 12 1986

✓ **S**

B

DEPARTMENT OF THE AIR FORCE
AIR UNIVERSITY

AIR FORCE INSTITUTE OF TECHNOLOGY

DTIC FILE COPY

Wright-Patterson Air Force Base, Ohio

86 2 12 05

AFIT/GAE/AA/85D-11

**An Experimental Study of Clustered Nozzles
with Variable Shrouds**

THESIS

**James R. Moran
Captain, US Army**

AFIT/GAE/AA/85D-11

**DTIC
ELECTE
FEB 12 1986
S D
B**

Approved for public release; distribution unlimited

AFIT/GAE/AA/85D-11

**An Experimental Study of Clustered Nozzles
with Variable Shrouds**

THESIS

**Presented to the Faculty of the School of Engineering
of the Air Force Institute of Technology**

Air University

**In Partial Fulfillment of the
Requirements for the Degree of
Master of Science in Mechanical Science**

James R. Moran

Captain, US Army

December 1985

Approved for public release; distribution unlimited

Preface

In selecting a thesis topic, I wanted to accomplish two personal goals. The first goal was to complete a thesis that would further a body of knowledge. The second goal was to engage in a project that involved a practical application of theories encountered in class instruction. An experimental thesis in clustered nozzles was selected to achieve these objectives.

The successful completion of this project would have been impossible without the advice and guidance of my thesis advisor, Dr. W. C. Elrod. He provided not only technical knowledge but was also an enjoyable person to work with and made the project a pleasure to work on. My admiration and respect for Dr. Elrod will last long past my tour at AFIT.

I would like to thank the aeronautical and astronautical technicians for their support throughout my thesis. Mr Nick Yardich, Jay Anderson and Leroy Cannon were invaluable in arranging for logistic support, running the experiments and solving technical equipment and instrumentation problems. The AFIT fabrication shop was responsible for construction of the test section and nozzle blocks. I would like to recognize Tim Handcock, for his work in building the equipment, and the contributions of Carl Shortt, John Brohas and Jack Tiffany.

This thesis would not have been possible without the loving sacrifices and support of my wife and family during the past 18 months. In closing, I would like to say that through God all this has come to being and I thank and praise him for his many blessings.

James R. Moran

Table of Contents

	Page
Preface	ii
List of Figures	v
List of Tables	vii
List of Symbols	viii
Abstract	ix
I. Introduction	1
Theory.....	2
Objectives	4
II. Experimental Apparatus	5
Test Section	5
Flow System	7
Nozzles	7
Instrumentation	7
Schlieren System	12
III. Data Acquisition and Reduction System	14
IV. Experimental Procedure	22
Calibration	22
Test Procedure	22
V. Results and Discussion	26
Results	26
Nozzle Block A	27
Nozzle Block B	30
Nozzle Block C	31

Discussion	33
VI. Conclusions	43
VII. Recommendations	45
Bibliography	46
Appendix A	47
Appendix B	56
Appendix C	65
Vita	69

Accession For	
NTIS GRA&I	<input checked="" type="checkbox"/>
DTIC TAB	<input type="checkbox"/>
Unannounced	<input type="checkbox"/>
Justification	
By _____	
Distribution/ _____	
Availability Codes	
Avail and/or	
Dist Special	
A-1	



List of Figures

Figure	Page
1. Test Section.....	6
2. System Schematic.....	8
3. Two-Dimensional Nozzle Block Dimensions.....	9
4. Three-Dimensional Nozzle Block Dimensions.....	10
5. Schlieren System.....	13
6. Hardware Schematic	16
7. HP 6901S System	17
8. Data Flow Path	19
9. HP 6901S Menus	20
10. Transducer Null Adjustment Circuit	24
11. Base Plate and Channel Flow.....	29
12. Thrust Ratio for Nozzle Block A	36
13. Thrust Ratio for Nozzle Block B	37
14. Thrust Ratio for Nozzle Block C	38
A-1 Pressure vs Time for Configuration 1A.....	48
A-2 P_s and P_a vs Time for Configuration 1A.....	49
A-3 Pressure Ratio vs Time.....	50

A-4	Schlieren Photographs for Configuration 1A.....	51
A-5	Pressure vs Time for Configuration 2A.....	52
A-6	Schlieren Photographs for Configuration 2A.....	53
A-7	Pressure vs Time for Configuration 3A.....	54
A-8	Schlieren Photographs for Configuration 3A.....	55
B-1	Pressure vs Time for Configuration 1B.....	57
B-2	Schlieren Photographs for Configuration 1B.....	58
B-3	Pressure vs Time for Configuration 2B.....	59
B-4	Schlieren Photographs for Configuration 2B.....	60
B-5	Pressure vs Time for Configuration 3B.....	61
B-6	Schlieren Photographs for Configuration 3B.....	62
B-7	Pressure vs Time for Configuration 4B.....	63
B-8	Schlieren Photographs for Configuration 4B.....	64
C-1	Pressure vs Time for Configuration 1C.....	66
C-2	Pressure vs Time for Configuration 2C.....	67
C-3	Pressure vs Time for Configuration 3C.....	68

List of Tables

Table	Page
I. Test Instrumentation.....	15
II. Nozzle Characteristics.....	34

List of Symbols

A_e	nozzle exit area (in ²)
A_t	nozzle throat area (in ²)
AR	nozzle area ratio (A_e / A_t)
g_c	conversion factor = 32.17 (lbm-ft) / (lbf-sec ²)
M_e	exit Mach number
m	mass flow rate (lbm/sec)
P_a	tank back pressure (psia), { P_5 }
P_c	chamber pressure (psia), { P_6 }
P_e	nozzle exit pressure (psia)
P_1	top exit plane pressure (psia)
P_2	top center exit plane pressure (psia)
P_3	bottom center exit plane pressure (psia)
P_4	bottom exit plane pressure (psia)
PR	pressure ratio (P_c / P_a)
T	thrust
U_e	nozzle exit velocity (ft/sec)
T_d	thrust for nozzle design
T_s	thrust with shroud

ABSTRACT

This research involved the investigation of pressure and flow fields in the base region of clustered nozzles during cold flow testing. Nozzle exit conditions simulating altitudes up to 75,000 feet and chamber-to-back pressure ratios up to 200 were used. The nozzle clusters considered were made up of sets of two and three dimensional supersonic convergent-divergent nozzles with a square shroud around the cluster. The two dimensional nozzles had design exit Mach numbers of 3.68 and 2.94. The three dimensional nozzles had a design exit Mach number of 2.64. The nozzle clusters were studied using various configurations and with two shroud lengths. A schlieren system that allowed for both still photographs and motion picture film was used to investigate the flow fields.

The results of this study indicate that the pressure fields in the base region of a nozzle cluster are dependent on both geometry and on the operating altitude. The outer wall of the test section (shroud) adjacent to the nozzles was observed to significantly affect the flow patterns and measured pressures. Potential influences in performance exist due both to changes in the gas dynamics of the flow and the appearance of additional pressure-area forces.

AN EXPERIMENTAL STUDY OF CLUSTERED NOZZLES WITH VARIABLE SHROUDS

I INTRODUCTION

The concept of grouping multiple rocket motors into a cluster arrangement has been examined for almost three decades. Early work by Goethert (2) in conjunction with the testing of the Polaris missile suggested the possibility of increased performance due to clustering. Previous AFIT studies by, Lester (6) and Bjurstrom (1) examined the potential performance effects of nozzle clusters due both to exhaust plumes interacting and plume interaction with a surrounding aerodynamic shroud.

This potential for increased performance may lead to new designs incorporating clustered nozzles. Additional research is necessary to understand what is occurring within the exhaust flow field of clustered nozzles in order to predict and exploit any possible performance augmentation. One example of a possible near future application is the work that is being done at the Air Force Rocket Propulsion Laboratory (AFRPL) in support of a Space Sortie Vehicle. This reusable system would be able to deliver small payloads to low orbit after being launched from a modified transport type aircraft. For aerodynamic reasons, and in an effort to speed development, use of a clustered arrangement of existing rocket engines is being considered. It is anticipated that performance may

be affected both by the interaction of the exhausts with each other and with a shroud that is under consideration.

Theory

Using conservation of momentum, a relation for nozzle thrust can be developed that states:

$$T = mU_E/g_c + (P_E - P_A)A_E \quad (1)$$

where

T = thrust (lbf)

m = mass flow rate (lbm/sec)

U_E = exit velocity (ft/sec)

P_E = exit pressure (psi)

A_E = nozzle exit area (in)

g_c = conversion factor

$$= 32.17 (\text{lbm-ft}) / (\text{lbf-sec}^2)$$

From this relation, it is evident that thrust can be expressed as the sum of two different phenomena. The first term is the product of the mass flow rate and the gas exhaust velocity with respect to the vehicle (6:25). This factor is the thrust due to the momentum flux and is the larger of the two terms. The second half of the expression is a pressure area term, often referred to as the pressure thrust. This additional force, usually small compared to the momentum flux when the engine is operating near design altitude, will be present in a supersonic nozzle whenever the gas

exit pressure is different from the ambient pressure. Further, the effect is sometimes sizable as demonstrated in the case of the Space Shuttle main engine which has a thrust of 375,000 lbf at sea level and a thrust of 470,000 lbf in vacuum. Overexpansion at sea level causes a pressure drag or negative thrust; while in a vacuum a pressure thrust or positive contribution is encountered.

If the pressure at the nozzle exit is less than the local ambient pressure an oblique shock pattern is generated to adjust the two pressures and the exhaust jet contracts downstream (4:410-411 ; 8:56-61). This situation is referred to as overexpanded flow and contributes a negative pressure area term or a decrease in thrust as is the case of the Space Shuttle engine at sea level. The converse situation develops when the exit pressure exceeds ambient pressure and is termed underexpanded flow. In this region, expansion waves occur at the nozzle exit and the jet will expand outward. In this situation, the pressure-area thrust contribution is positive as is the case of the Space Shuttle engine operating in a vacuum. In each of these cases alternating sets of compression and expansion waves (a diamond pattern) occurs to alleviate the pressure mismatch condition at the nozzle exit. A third case is the perfectly expanded nozzle where the two pressures are equal. This optimal situation will exist only at one altitude for a fixed chamber pressure (i.e., the design altitude) as the vehicle ascends and results in no spreading or contracting of the plume.

The exit area (A_e) can be increased to a larger effective area by the addition of a shroud around the nozzle(s). If the flow expands to the

shroud a larger effective A_e results with an accompanying increase of the thrust. The larger effective A_e influences the nozzle performance characteristics by altering the area ratio (A/A^*), exit Mach number and the pressure ratio (P_c/P_e).

Objectives

Previous AFIT thesis work done by Hibson (3), Lester (6), and Bjurstrom (1) studied the effects of clustering on the performance of rocket engine nozzles. In this project an experimental apparatus was established to examine clustered nozzles under conditions found at high altitudes with these specific objectives:

1. To configure an automated digital acquisition and reduction system, including software development, which replaces the visicoder used in all previous nozzle cluster research done in this area at AFIT.
2. To experimentally analyze the pressures encountered in the nozzle base region and estimate the effect on thrust due to the interaction of the nozzle exhausts.

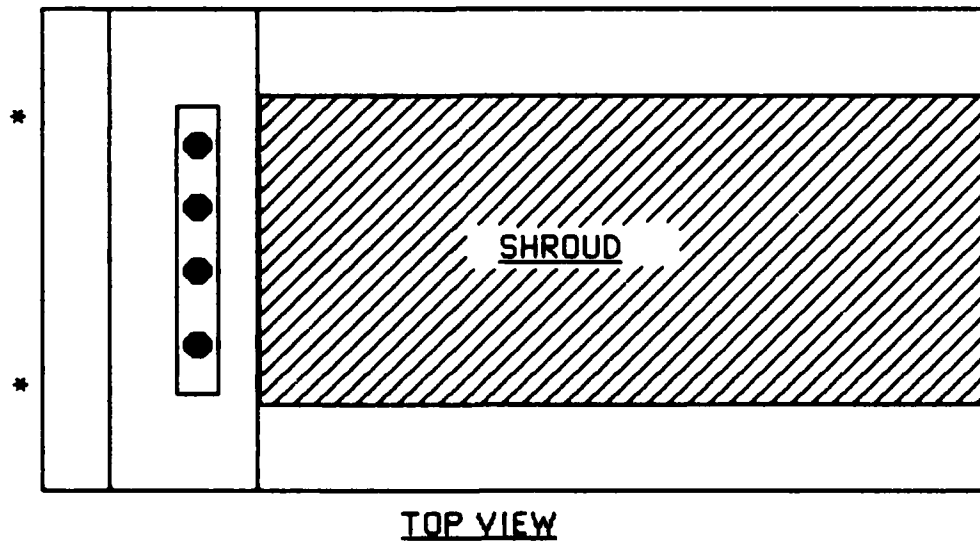
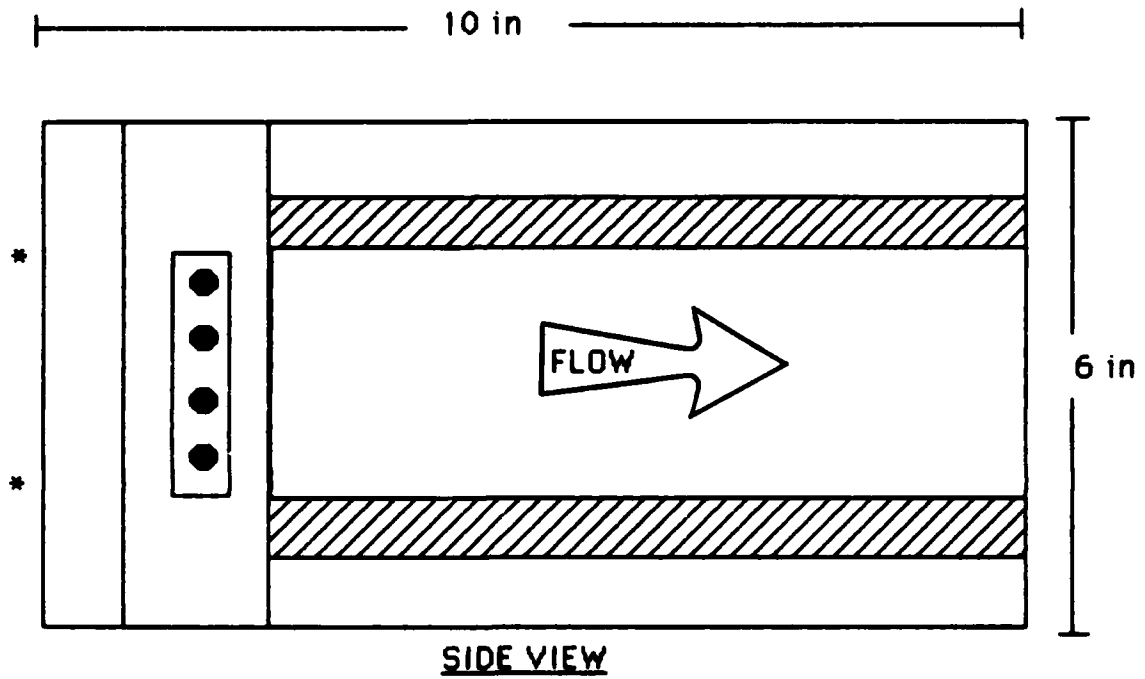
II EXPERIMENTAL APPARATUS

This investigation was conducted using the AFIT blowdown facility with the compressed air supplied to the test section being discharged into a vacuum chamber. Test articles investigated included two-dimensional and three-dimensional convergent-divergent nozzle clusters. An automatic data acquisition and reduction system, which will be described in Chapter III, was developed to enhance the research. A primary consideration was the need to automate the data acquisition and reduction process.

The equipment was designed to accommodate a variety of test blocks thereby permitting a wide range of differing geometries to be studied. In particular; by varying nozzle shapes, nozzle firing patterns and shroud lengths any number of possible vehicle configurations may be simulated.

Test Section

The test section (Figure 1) consisted of a nozzle cluster as depicted in Figures 3 or 4 and a flow channel. The nozzle blocks were inserted into the test section and the sides of the test section provided the shrouded flow channel. The shroud sides were optical glass to allow for schlieren photographs and motion pictures of the flow patterns. The top and bottom plates of the shroud were removable so that various shroud lengths could be investigated. The shroud dimensions formed a 2 inch square flow channel downstream from the nozzle cluster.



● Transducer Mount

- Nozzle Block mounting orifice

Figure 1. Test Section

Flow System

Compressed air at 95 psi was supplied by a 100hp compressor and delivered via a three inch line through a hand operated valve into a stilling chamber (Figure 2). The chamber design assured that a uniform air flow was provided to the test section. The test section was installed in a large tank connected to the vacuum system. Ten inch square optical quality glass windows were mounted into the sides of the large tank to allow for schlieren photographs of the flow as it was exhausted from the nozzles. To remove both particles and moisture from the air supply an internal paper-type filter was included.

Nozzles

Three different nozzle clusters were studied. Two of the nozzle blocks were two-dimensional sets of three nozzles (Figure 3). One had a throat-to-exit area ratio of 1:4 and the other was 1:8. Inserts were also made so that two of the nozzles could be plugged. This allowed for analysis of the nozzle block with either all three or just one of the nozzles flowing. The other nozzle cluster was a three-dimensional nozzle as shown in Figure 4. These nozzle block configurations also had the capability of blocking any one or more of the nozzles with o-ring mounted inserts. The critical dimensions of all nozzle blocks and nozzles mounted therein are depicted in Figures 3 and 4.

Instrumentation

Six pressure transducers were used to record data. In the two-dimensional configurations, four Endevco model 8510-10B

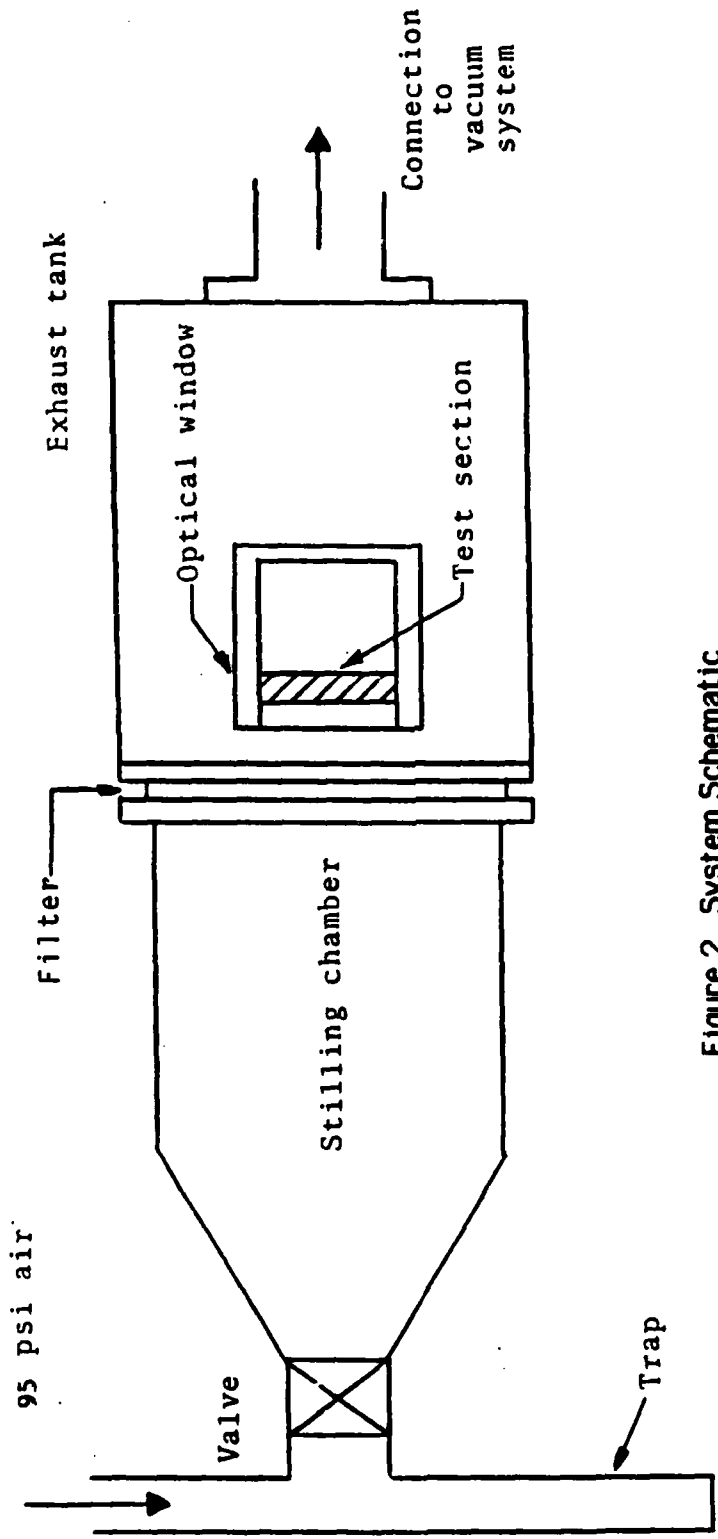
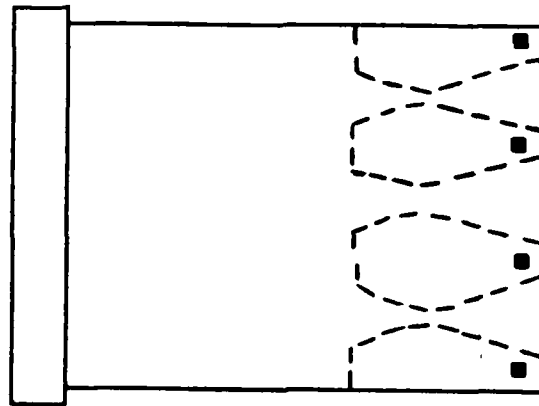
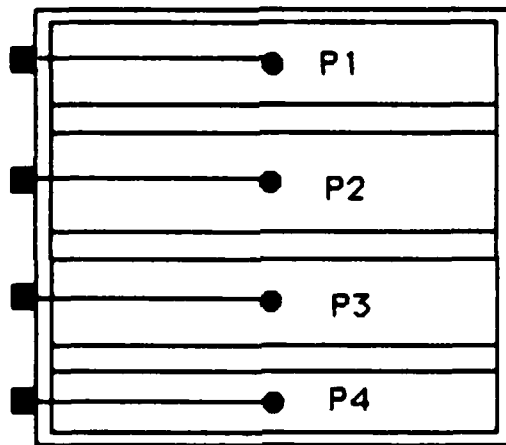


Figure 2. System Schematic



PROFILE



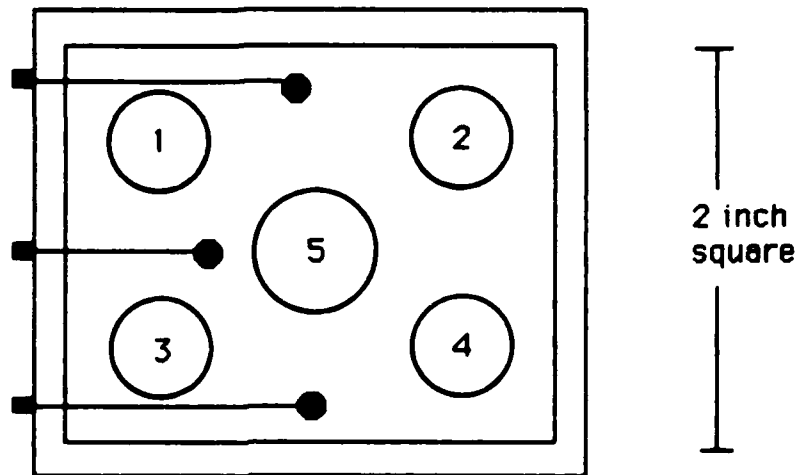
2 inch
square

FRONT

Nozzle Set	Throat Width	Exit Width
A	0.05 inch	0.40 inch
B	0.05 inch	0.20 inch

- Transducer Mount
- Measurement Station

Figure 3. Two-Dimensional Nozzle Block Dimensions



NOZZLE	A_t (in ²)	A_e (in ²)
1-4	0.1520	0.456
5	0.2206	0.6618

- Transducer Mount
- Measurement Stations

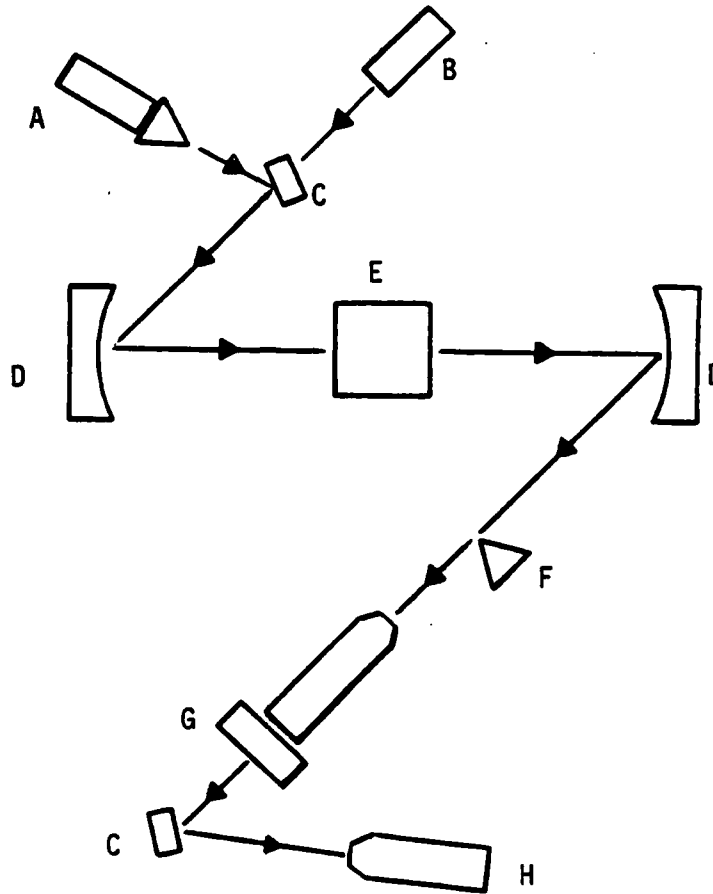
Figure 4. Three-Dimensional Nozzle Block Dimensions

piezoresistive transducers measured the exit plane pressure above, between and below the nozzles (P_1 , P_2 , P_3 , P_4 respectively). The three-dimensional configurations employed three transducers. The measuring stations are shown in Figures 3 and 4. A fifth transducer (P_5) of the same make and model was used to measure the downstream or back pressure of the large tank downstream of the test section. All five of the Endevco model 8510's had a range of ± 10 psi. These differential transducers were connected to a separate vacuum pump that generated a vacuum as a reference pressure. The sixth transducer was an Endevco model 8530. This transducer had a 0-100 psia range and measured the upstream or stagnation pressure (P_6). It was located just aft of the paper filter and forward of the test section.

In addition to the transducers, two mercury manometers were used during the test and calibration runs. One was connected to the stilling chamber and a second to the large tank for measuring downstream pressures. Since the manometers had a 50 psi limit and the chamber pressure would approach twice that, a bourdon tube pressure gage with a 200 inch Mercury range allowed for calibration through the entire pressure range. To facilitate transducer calibration, a 0.25 inch outside diameter line was connected from the 95 psi air supply through a small valve into the stilling chamber. Calibration was accomplished using this air supply since it allowed for incremental adjustment of the chamber pressure.

Schlieren System

One of the objectives of the experiment was to study the nozzle exhaust-shroud flow patterns as conditions changed from the underexpanded to overexpanded regimes. To study these quasi-steady flow conditions a schlieren system was devised that allowed for motion pictures as well as still pictures. For still pictures, Polaroid sheet film was used in conjunction with a spark lamp with a duration less than 1 micro-second. A steady light source was used for recording the entire run on 16 mm film. To supplement the pressure data several runs with each nozzle block configuration were filmed. Figure 5 depicts the schlieren system used.



- A. Steady light source (motion pictures)
- B. Spark lamp (still photos)
- C. Flat mirror
- D. Concave mirror
- E. Test section
- F. Knife edge
- G. Still camera (still photos)
- H. Film or video camera (motion pictures)

Figure 5. Schlieren System

III DATA ACQUISITION

One of the major objectives of this study was to replace the Honeywell visicoder used in previous work with this facility with a automated digital system. The automatic data acquisition and reduction system was developed to compliment the facility and enhance the research. The experimental apparatus was also designed to automate the data acquisition and reduction process. The hardware components listed in Table I were selected to accomplish the objective and were subsequently configured according to Figure 6. All component links were made with the HP interface bus.

The center of the data collection process is the HP 6901S Measurement and Analysis System. This system provides a multi channel data acquisition and conversion system capability. It is configured to collect data from 264 channels in either analog or digital form. The sampling capacity of the system with a full complement of interface cards is 100,000 samples per second. While this investigation did not require the entire range of the system it did significantly upgrade the facility for this study and future applications. A simplified functional diagram of how the HP 6901S interfaces with the other operational devices is shown in Figure 7.

The Measurement and Analysis System is designed to have a HP 6942 Multiprogrammer internally mounted. The Multiprogrammer contains the memory cards, analog to digital converters, scanner relays and controller cards for system operation. Data is acquired through the

Table I Test Instrumentation

<u>Item</u>	<u>Model #</u>	<u>Serial #</u>
Pressure transducer (P ₁)	Endevco 8510	PP81
Pressure transducer (P ₂)	Endevco 8510	PP82
Pressure transducer (P ₃)	Endevco 8510	PP75
Pressure transducer (P ₄)	Endevco 8510	PP79
Pressure transducer (P ₅)	Endevco 8510	PP70
Pressure transducer (P ₆)	Endevco 8530	TM83
Power supply	HP 6205B	1949A1663
Multiprogrammer	HP 6942A	2513A-06003
Computer	HP 9826	2313A05860
Plotter	HP 7470A	97468
Printer	HP 9871A	1537A09303
Measurement and Analysis Sys	HP 6901S	2342A-00104

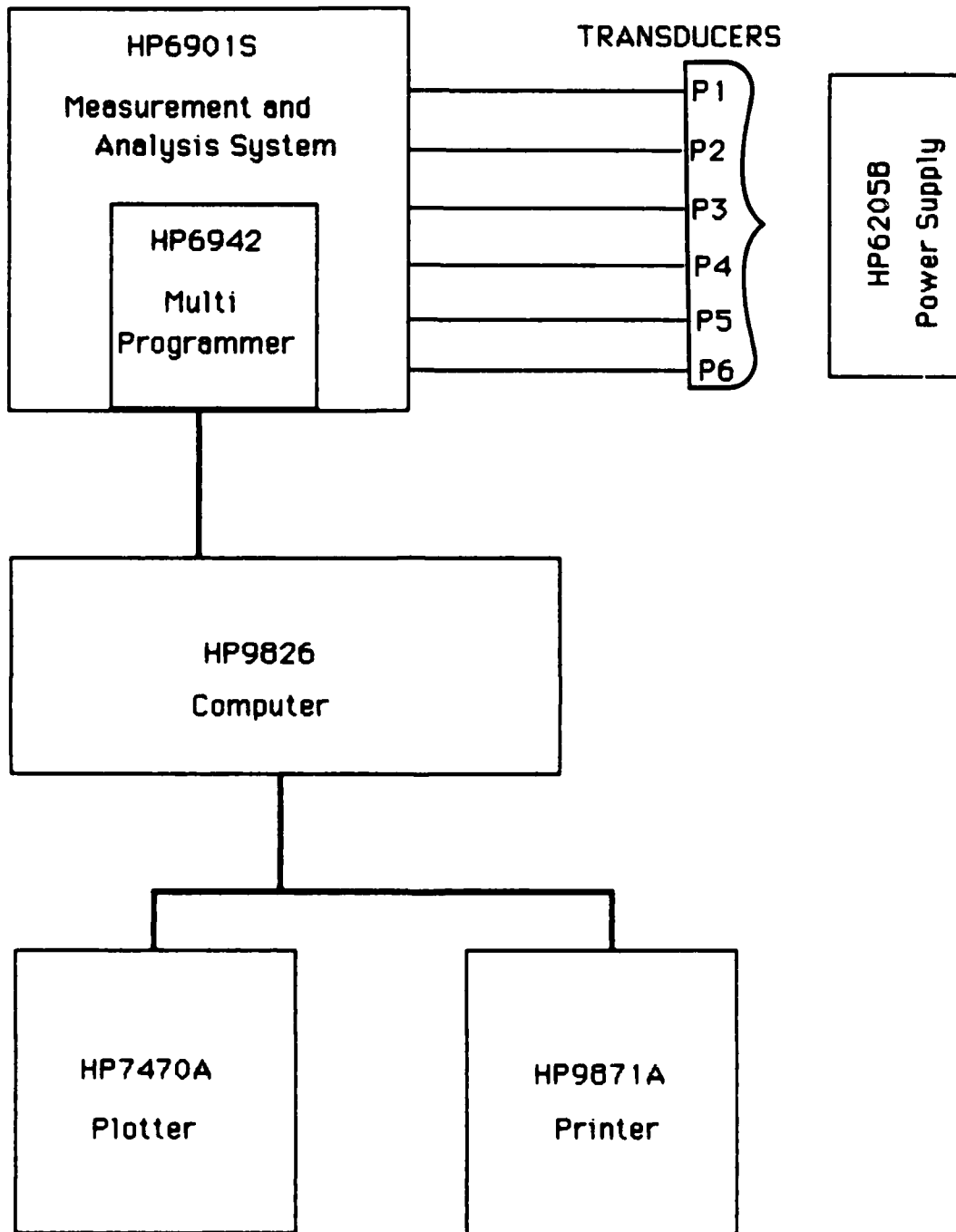


Figure 6. Hardware Schematic

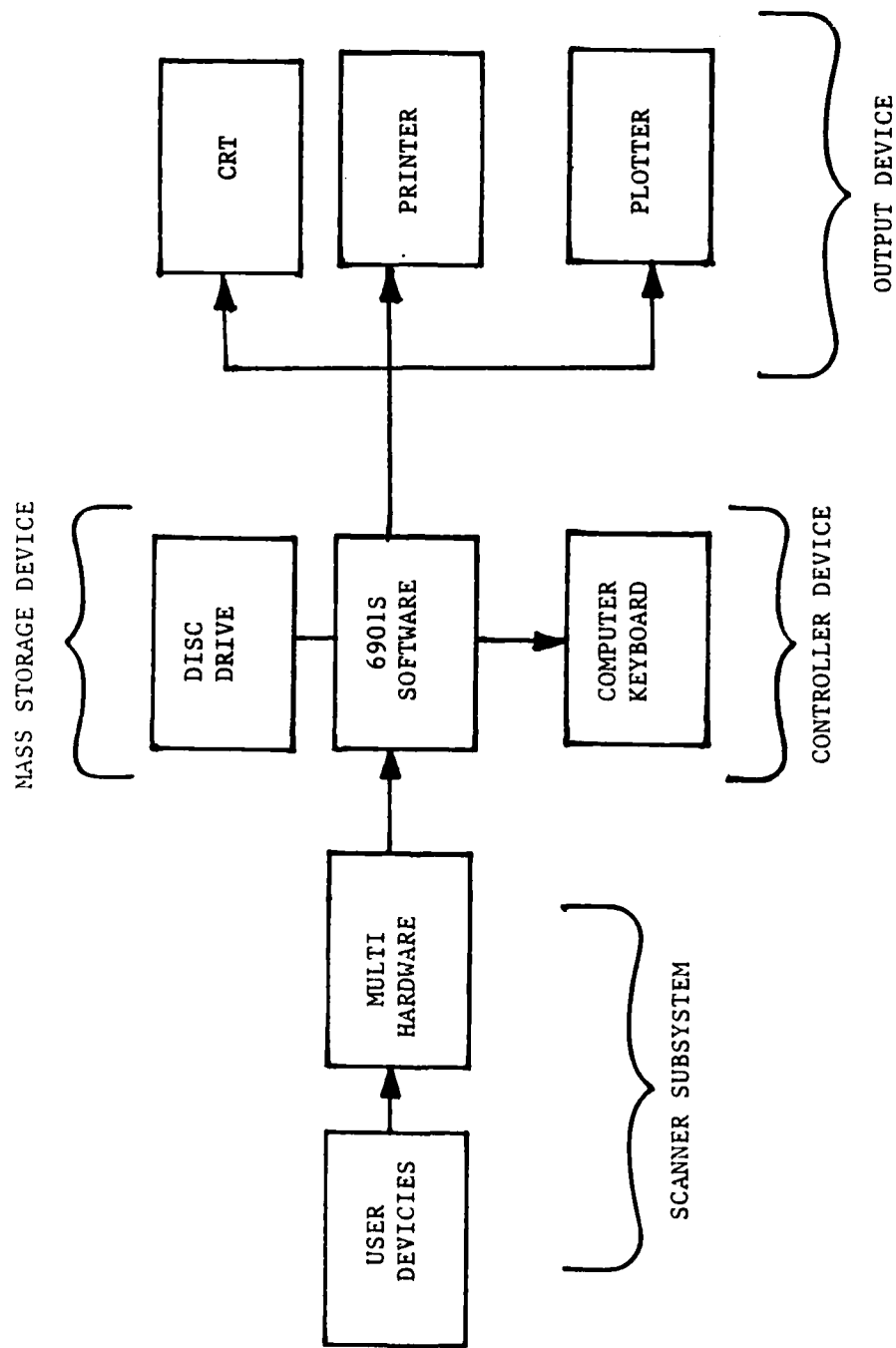


Figure 7. Simplified Functional Diagram of 6901S System

terminal boards contained on the HP 6901S and is temporarily stored. Storage of the data is required to achieve the sampling capacity while not overloading the conversion capability of the analog to digital converters. The data is recalled from temporary storage in sequential order processed into digital form and then sent to the HP 9826 computer. The general data flow path is shown in Figure 8.

The HP 9826 computer and accompanying software for the HP 6901S is menu drive system (Figure 9). The menus were executable commands for control and a vehicle to enter experimental parameters. The computer, like the HP 6901S, with a one megabyte capacity was more than capable of controlling the experiment with sufficient computational ability. The test run data acquisition parameters including sample rate, sample duration, and sample time were entered via a modified HP 6901S software package. For this study the software was set to sample all channels every 0.1 seconds and had a time interval of 1600 microseconds for each successive channel and total sample time of 30-60 seconds depending on the nozzle configuration. The software package also allowed for a selection from various data presentation formats (table, graph or histogram). The data reduction equations (calibration equations and offset points) were implemented by the computer prior to the presentation of any output format.

Several programs were written to reconfigure the data presentation formats. These plotting programs load the file containing the data by assigning I/O paths to refile the transformed presentation. The new file is then plotted on the HP 7470A Plotter. These programs were designed with flexibility for various possible alternatives in

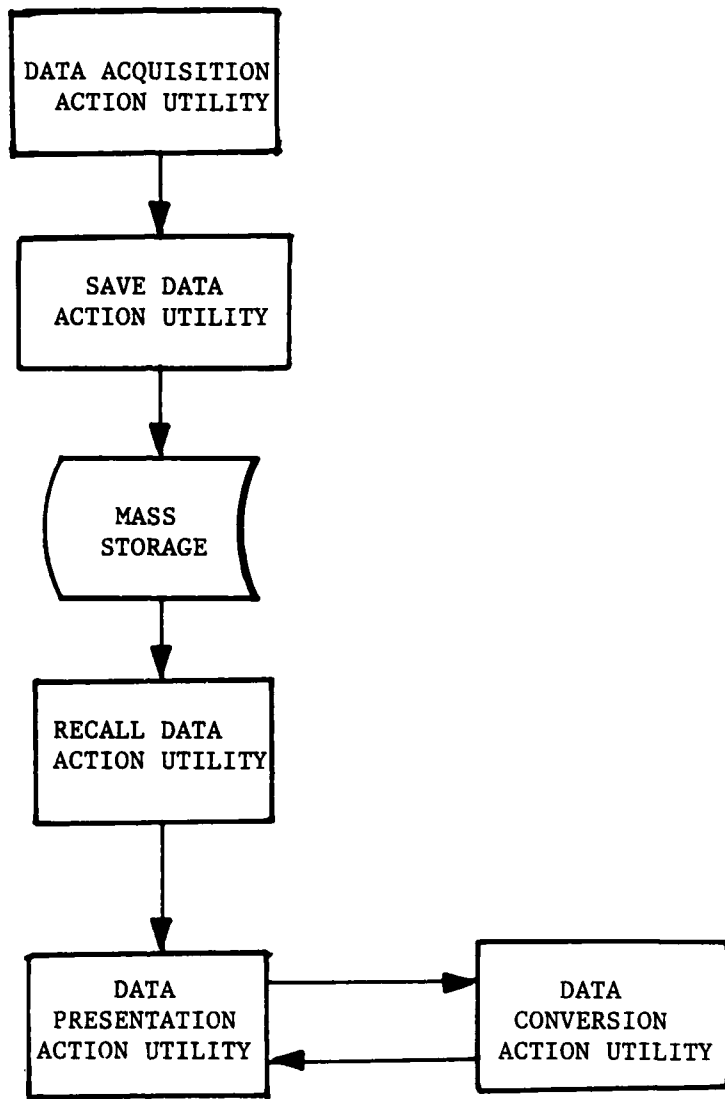


Figure 8. Data Flow Path

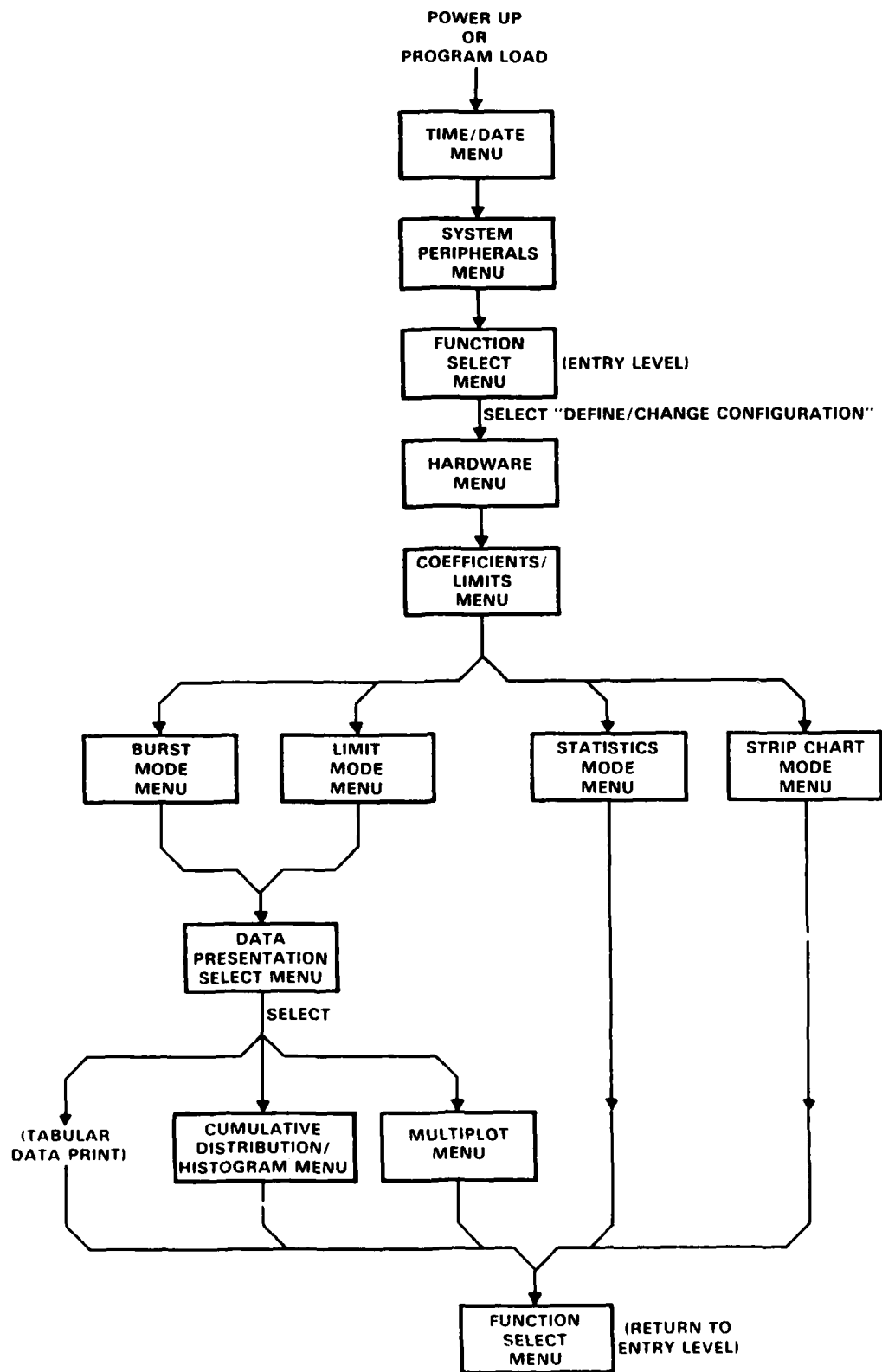


Figure 9. Operational Flow Diagram of 6901S Menu Utilities

formatting.

The data acquisition and reduction system was suitable for research on the blowdown facility. The essential performance characteristics of the test section and nozzle clusters were adequately acquired, processed and formatted. The system is also expandable and adaptable for future research on the facility. However, if future work is to include more complex computational equations, a Fortran or Pascal compiler should be added to enhance numerical processing.

IV EXPERIMENTAL PROCEDURE

Calibration

All of the Endevco 8510 transducers (P1-5) were calibrated in place on the apparatus. The transducers were connected to a separate vacuum pump that established a reference pressure of approximately 0.01 psia. The main vacuum pumps were used to lower the vacuum-chamber pressure to values within the transducer's range above the reference pressure. These transducers would then generate a voltage corresponding approximately to absolute pressure. A digital voltmeter was used to record the transducer output voltage while a mercury manometer indicated the pressure. The slope of the pressure versus voltage curve was used to determine the sensitivity of the transducer.

The chamber pressure transducer (P_G) was calibrated using a separate test device. This transducer measured absolute pressure (psia) so the need for a separate vacuum pump was eliminated. The transducer was mounted in the block with a 100 psi regulated source. The source was also connected to a 100 inch mercury manometer. The pressure was varied using the regulator and the voltage recorded. Since the pressure gauge agreed very closely with the manometer in the zero to 50 psig range it was assumed that the gauge was also accurate up to the maximum chamber pressure of approximately 100 psia. All transducers were connected to a 10 volt power supply during both calibration and testing.

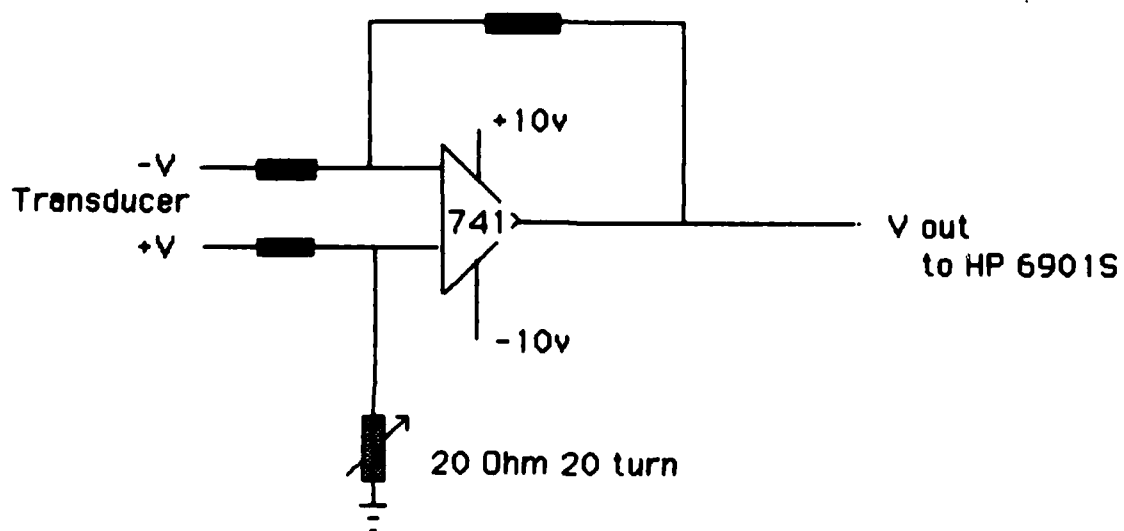
Test Procedure

The basic procedure on all the test runs was the same. First, each of

the air valves including the main valve into the stilling chamber were closed. All of the associated electronics were turned on and the excitation voltage for the pressure transducers was set to 10 volts DC. Using the circuit shown in Figure 10, each transducer output was adjusted to the null position. This circuit was necessary to reduce the background noise by using the differential amplifiers arranged in a system with a gain of one. The common mode rejection characteristics of this circuit with its associated gain preserved the signal while at the same time producing a cleaner transducer output. The multiprogrammer and computer system were turned on and the appropriate software programs were loaded. These included the data acquisition and reduction programs. Then, the two main vacuum pumps were used to establish the desired initial downstream conditions. Since on each run this downstream pressure would vary continuously, thus providing a changing overall pressure ratio, it was normal to establish the lowest starting back pressure possible. Due to small leaks within the system this initial value was limited to approximately 0.25 psia.

Once the initial conditions were established, the test run was started. At the computer's programmed command the air supply valve was opened to supply pressure to the system. After the desired test time was complete the valve was closed and the supply air was cutoff. The computer stored the data and the reduction program was used to convert the data to useful pressure versus time graphic outputs.

Data from the pressure transducers were recorded with the HP 6901S Measurement and Analysis System and the HP 9826 Computer for a number of test runs for each nozzle set. At each point where an abrupt change of




 > 10 Ohm resistor

FIGURE 10. Transducer Null Adjustment Circuit

flow conditions was encountered additional runs with initial ambient pressure both above and below where the phenomenon occurred were accomplished. This procedure of using different starting back pressures indicated there were virtually no prior history effects involved in this experiment. That is, the changes of flow conditions occurred at the same pressure ratios regardless of what the starting condition was. The vacuum pump capacity was not adequate to check for hysteresis in the pressure ratio for flow condition changes by increasing the pressure ratio during the run.

V RESULTS AND DISCUSSION

Results

The behavior of the exhaust of a single supersonic nozzle in both underexpanded and overexpanded flow is well established (4:410-411). When two or more nozzles operate in close proximity or in close proximity to a shroud, additional phenomena arise in the flow patterns. Common in both of the two dimensional nozzles was the attachment and interaction of the flow with the shroud and with each other.

The concept of each nozzle acting at a larger effective nozzle expansion ratio results in an increase of the momentum thrust term. The schlieren photographs for this study show that the flow continues to expand after the primary nozzle exit plane until it attaches to the shroud. Bjurstrom (1) noted this effect in one of his nozzles assemblies. Goethert (2) suggested individual cylindrical shrouds for each three-dimensional nozzle in which case the interaction of the flow streams with each other would not occur until beyond the exit plane of the shrouds. For configuration A and B of this study the expansion ratio becomes 1:13 for all three nozzles flowing and 1:40 for the center only case when the flow attaches to the shroud. The change in the area ratio resulted in an increase in the exit Mach number.

An ascending rocket operates in a decreasing ambient pressure from the relatively high sea level conditions to the near absolute vacuum of the upper atmosphere. The resulting increase of chamber to ambient pressure ratio is the reverse of what was generated within the laboratory

apparatus. Ambient pressure in the experimental case was initially low and increased throughout the test run as the vacuum chamber pressure increased.

The flow began with the nozzle in the underexpanded region. As the backpressure passed the nozzle design altitude of 60,000 feet the individual nozzles would have transitioned into the overexpanded region. However, the initial conditions were established with the nozzle in the underexpanded region with the jets attached to the shroud and adjacent jets interacting. This isolated the nozzle exit plane from the outside effects for some period of time. The duration and nature of the attachment and interaction were dependent on geometric considerations. The pressure versus time histories and schlieren photographs are presented in Appendices A thru C. Each Appendix contains the results for a nozzle block configuration including the particular nozzle flowing and the shroud lengths investigated.

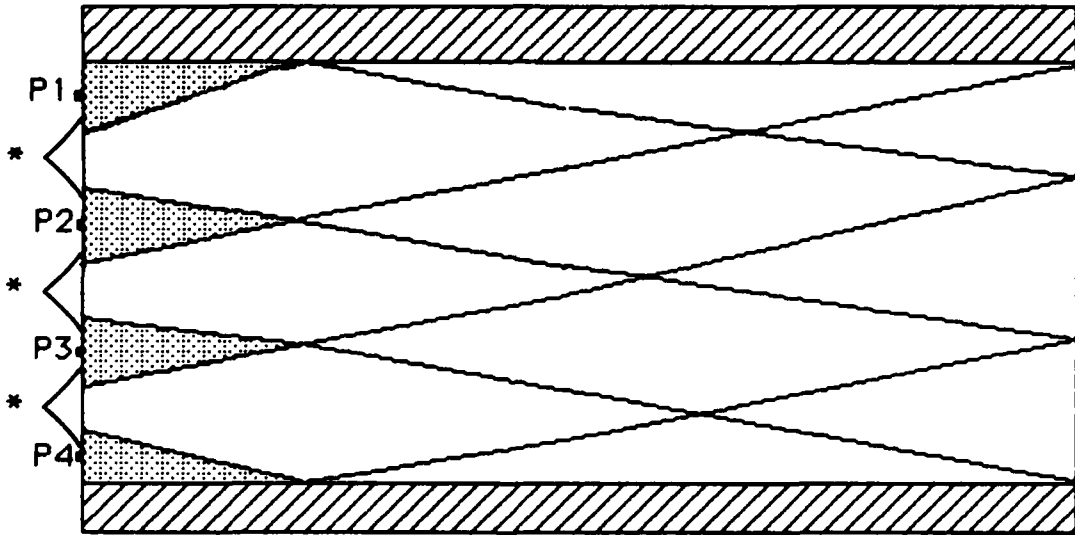
Nozzle Block A

Nozzle block A had an throat area to exit area ratio, A_t / A_e , of 1:8 (Figure 3). This nozzle block was run in a total of four configurations. The first two configurations of the nozzle block were run with all three nozzles flowing. Data was taken to examine the nozzle block performance when employing both a short and long shroud. The process was repeated with only the center nozzle of the nozzle block flowing. The same long and short shrouds were used as when all three nozzles were flowing.

In configuration 1A the nozzle block had all three nozzles flowing

with the long shroud. The flow began with the three jets interacting and flowing straight downstream. The interaction of the flow is characterized by the a distinctive diamond pattern exhibited in Figure A-4. As the test run progressed the pressure ratio (P_c/P_a) steadily decreased (Figure A-3). Figure 11 shows how the expanding flow separated the base region into four enclosed areas. When the pressure ratio reached PR=20, pressures P_1 and P_4 increased (Figure A-1) as a result of the flow pattern breaking away from the shroud. These pressures continued to increase until the run was terminated at 25 seconds. Pressure P_3 increased slightly as the backpressure continued to increase as seen in Figure A-1.

In configuration 2A with the short shroud, the pressure ratio (P_c/P_a) behaved in the same manner as configuration one. With the shorter shroud a more pronounced change occurred for the top and bottom pressure transducers, P_1 and P_4 , at the point of flow detachment from the shroud. When PR reached 23 at 15 seconds into the test run, the flow detached from the shroud and P_1 increased accordingly (Figure A-5), P_4 followed the same pattern two seconds later. As the pressure ratio continued to decrease to PR=20, P_3 and finally P_2 increased as the diamond flow pattern dissipated. The dissipation of the diamond pattern was the result of the increasing backpressure. The schlieren photographs (Figure A-6) begin with the flow of the outer nozzles attached to the shroud and the flow between the nozzles interacting with each other. This combination of attachment and interaction account for the diamond pattern in the Figure A-6a. Flow detachment begins at the shroud exit and



 Base plate areas isolated from the backpressure by the flow expanding to the shroud.

 Shroud

* Nozzle exit plane

FIGURE 11. Base Plate and Channel Flow

moves towards the base plate as P_a increases as shown in Figures A-6b and c. At the completion of the test run the flow is highly turbulent and the interaction of the three jets begins to break down.

Nozzle Block B

This nozzle had an area ratio, A_t/A_e , of 1:4. The same configurations tested for Nozzle Block A were examined for this nozzle block.

Operation of configuration 1B began with the flow attached to the shroud (Figure B-2). The flow remained attached for 23 seconds, then as the pressure ratio approached PR=15, it detached from the top and bottom of the shroud allowing the pressure measured by P_1 and P_4 to increase (Figure B-1). Transducers P_2 and P_3 remained blocked from P_a throughout the test time.

Figure B-4, which shows the three nozzles flowing with the short shroud, provides an excellent pictorial description of the performance of configuration 2B. The flow begins with attachment to the shroud as in previous configurations. Then as the back pressure increases the diamond flow pattern is gradually replaced by a turbulent region. The flow on the P_4 transducer side detaches first at 15 seconds into the test run when the pressure ratio is PR=17. The pressure measured by P_1 increases next at a pressure ratio of PR=15. Pressures P_2 and P_3 rise at PR=13 and PR=14 respectively. Figure B-3 shows the performance of the nozzle block configuration in a pressure versus time graph.

Configuration 3B has only the center nozzle flowing with the short shroud. Figure B-6 shows the flow attached to both the top and bottom walls of the shroud. At 11 seconds into the test run when PR=74 the flow detaches from bottom wall and P_3 increases (Figure B-5). Four seconds later when PR=45, the pressure transducer at P_1 shows an increase because of the flow detachment from the top of the shroud.

Configuration 4B also had only the center nozzle flowing but it had the long shroud. Here also, the run began with the flow attached to the bottom and top of the shroud (Figure B-8). When the pressure ratio reached PR= 39 the flow detached and the pressures at P_1 and P_3 increased to the back pressure, P_a . Figure B-7 shows the performance characteristics of this configuration.

Nozzle Block C

Nozzle Block C was a three dimensional nozzle cluster of five nozzles (Figure 4). Test runs were made in three different flow configurations; center nozzle (1C), outer nozzles (2C), and all five nozzles flowing (3C). All three configurations were run with the long shroud.

Unlike the two dimensional cases, this nozzle flow pattern did not isolate the individual transducer ports. In the two dimensional configurations the diamond pattern cutoff the transducers from the ambient backpressure and from each other. In all the three-dimensional configurations the exit plane pressure was uniform and each transducer measured this pressure vs. time for the run. The distinguishing characteristics of each configuration was the pressure ratio in which the

flow detached from the shroud. In configuration 1C the flow had a pressure ratio $PR=46$ at the transition. In configurations 2C and 3C the flow had pressure ratios of $PR=16$ and $PR=12$ respectively when the flow detached and the transducer pressure readings increased. Figures C-1 through C-3 show the pressure versus time history of each of the clusters. Since all the transducers had the same readings, the figures represent the pressure values at all the transducer locations.

Discussion

The rationale for exploring both clustered nozzles and shrouds lies in an explanation for and a potential to exploit increased nozzle performance. Equation (1) showed that any added performance must come from either the pressure-area term or the momentum flux term. The results of this study and the study Geothert (2) suggest that each term of the equation may be affected by the clustering of nozzles as well as by the addition of a shroud. In this regime, addition of a shroud and thereby effectively increasing the nozzle expansion ratio may be beneficial to engine performance. Any added thrust caused by the interaction of the jets with each other and the shroud should be taken advantage of in rocket nozzle design. This potential is the greatest at higher altitudes where the rocket engine operates in the underexpanded regime.

A comparison of the theoretical performance of a nozzle with and without a shroud is contained in Table II. Isentropic flow was assumed in both cases. The increase in exit Mach number and overall design pressure ratio were the result of the AR increasing due the flow expanding to the shroud. It may be noted from the last column in Table II that in the configurations where all three nozzles were in operation (1A,2A,1B and 2B) the PR at which the flow began to detach from the shroud was lower than the design PR of the individual nozzles. However in the configurations where only the center nozzle was flowing ,3B and 4B, the PR when detachment started was higher than the design pressure ratio of the nozzle. In the three-dimensional configurations, as the number of nozzles flowing increased the PR at detachment decreased until it was

Table II. Theoretical Nozzle Characteristics

Config- uration	Nozzle			Nozzle w/ Shroud		
	A/A*	M	P_c/P_a	A/A*	M	P_c/P_t
1A	8	3.68	98.2	13.3	4.24	20
2A	8	3.68	98.2	13.3	4.24	23
1B	4	2.94	34.0	13.3	4.24	15
2B	4	2.94	34.0	13.3	4.24	17
3B	4	2.94	34.0	40.0	5.65	74
4B	4	2.94	34.0	40.0	5.65	39
1C	3	2.64	22.0	26.3	5.05	46
2C	3	2.64	22.0	6.6	3.47	16
3C	3	2.64	22.0	4.8	3.13	12

(t) transition P_a

lower than the nozzle design value. This was the case in configurations 2C and 3C where the design PR was 22 but the detachment transition PR's of the nozzle with shroud shown in the P_c/P_t column of Table II were 16 and 12 respectively.

An additional relationship was discovered between shroud lengths of the two-dimensional nozzle blocks when examining the PR at detachment. When the short shroud configuration 2A was compared to the long shroud configuration 1A, the PR at which flow separated from the shroud occurred was 13 percent less for the short shroud configuration. A comparison of this relationship of the shroud length to the detachment PR in the configurations of 1B and 2B yielded a similar change of PR of 12.24 percent. The effect of differing shroud lengths when only the center nozzle is flowing was the same but the difference in PR's was closer to 50 percent. The relationships between the shroud lengths and the PR for flow separation from the shroud, and the number and geometry of nozzles in the cluster should be investigated further for any possible advantages in performance characteristics.

The isentropic thrust with and without a shroud for increasing ambient pressure was computed for each nozzle block. Results are contained in Figures 12 (Nozzle Block A), 13 (Nozzle Block B), and 14 (Nozzle Block C). For all nozzle blocks, as the number of nozzles in the block was increased, the slope of the thrust ratio was smaller than with fewer nozzles. For example in Figure 10, the initial condition thrust ratio begins at 1.15 for one nozzle and decreases to equality at 400 psf, but the three nozzle configuration decreases only from a T_s/T_d of 1.10 to 1.07.

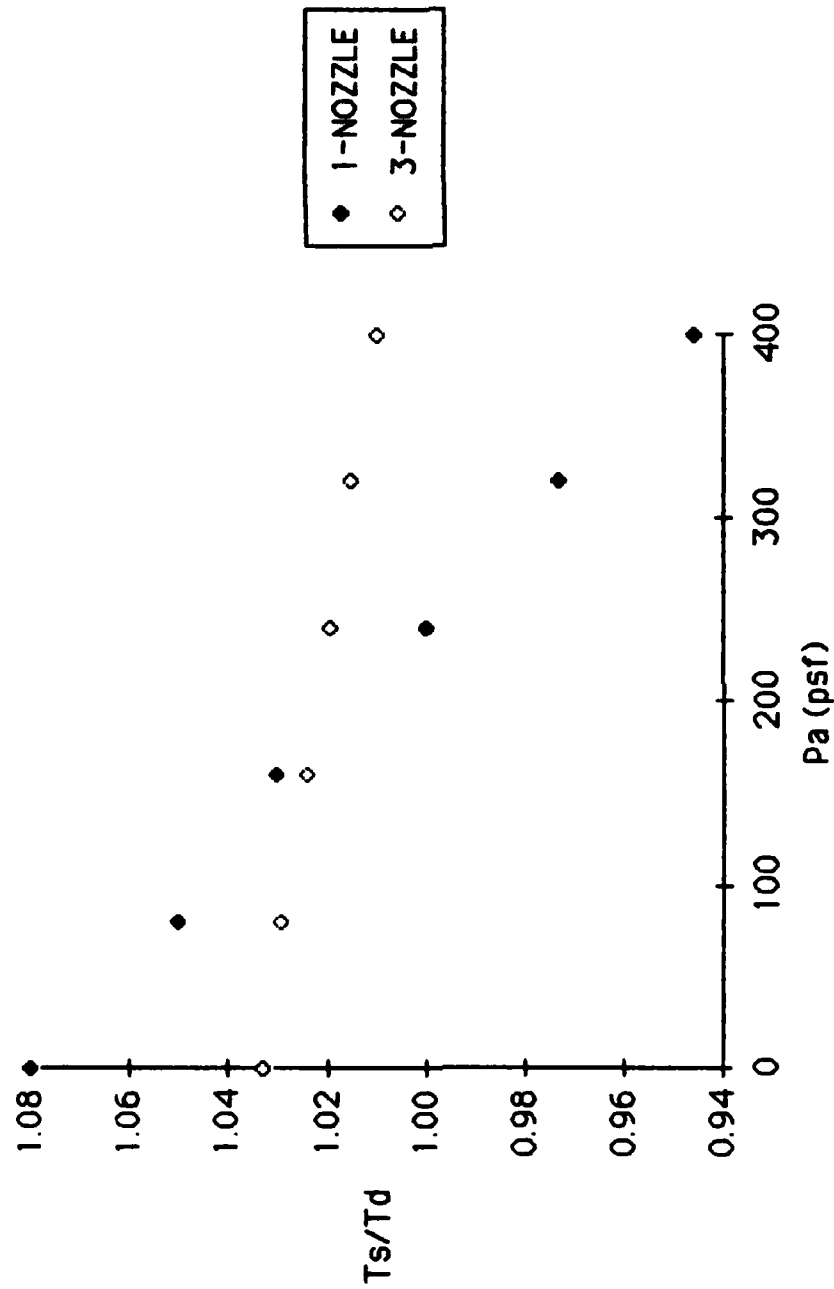


FIGURE 12. NOZZLE A THRUST RATIO

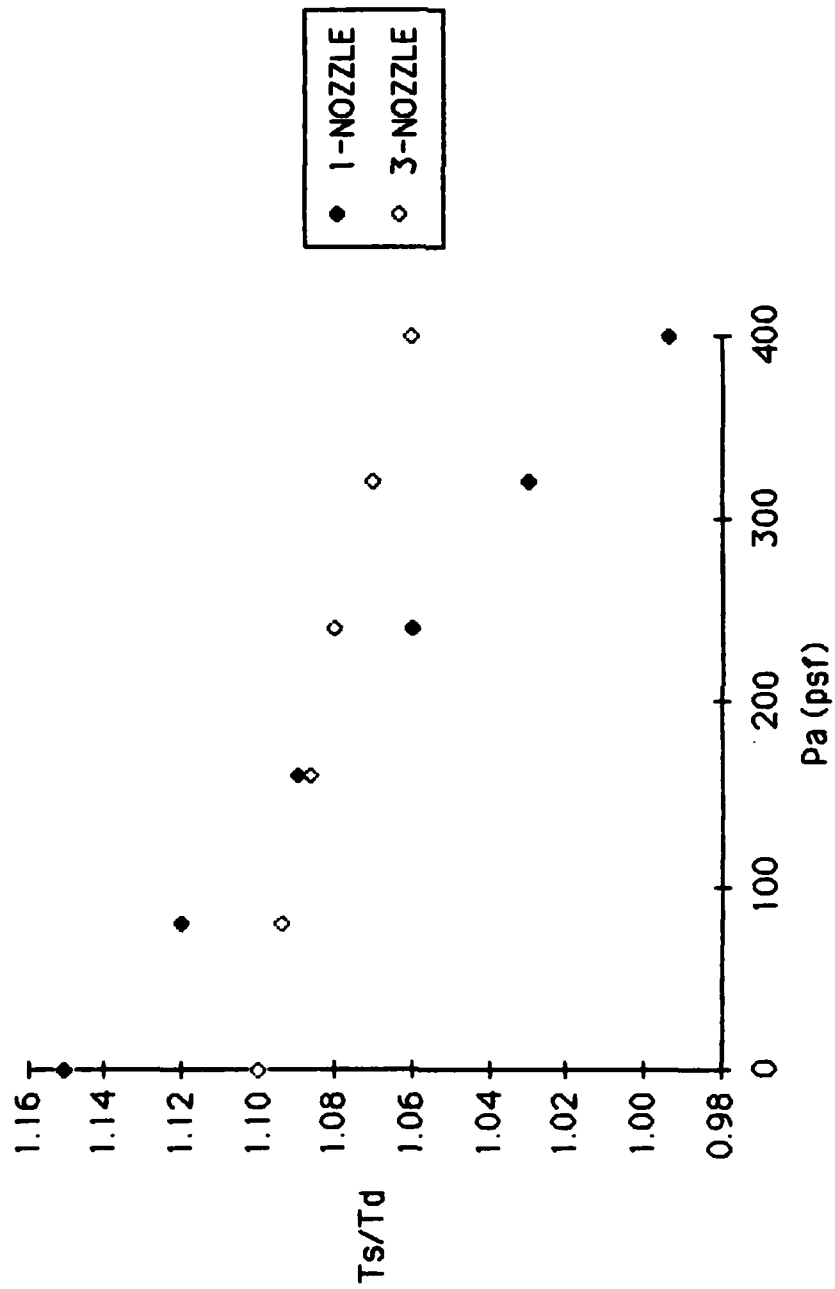


FIGURE 13. NOZZLE B THRUST RATIO

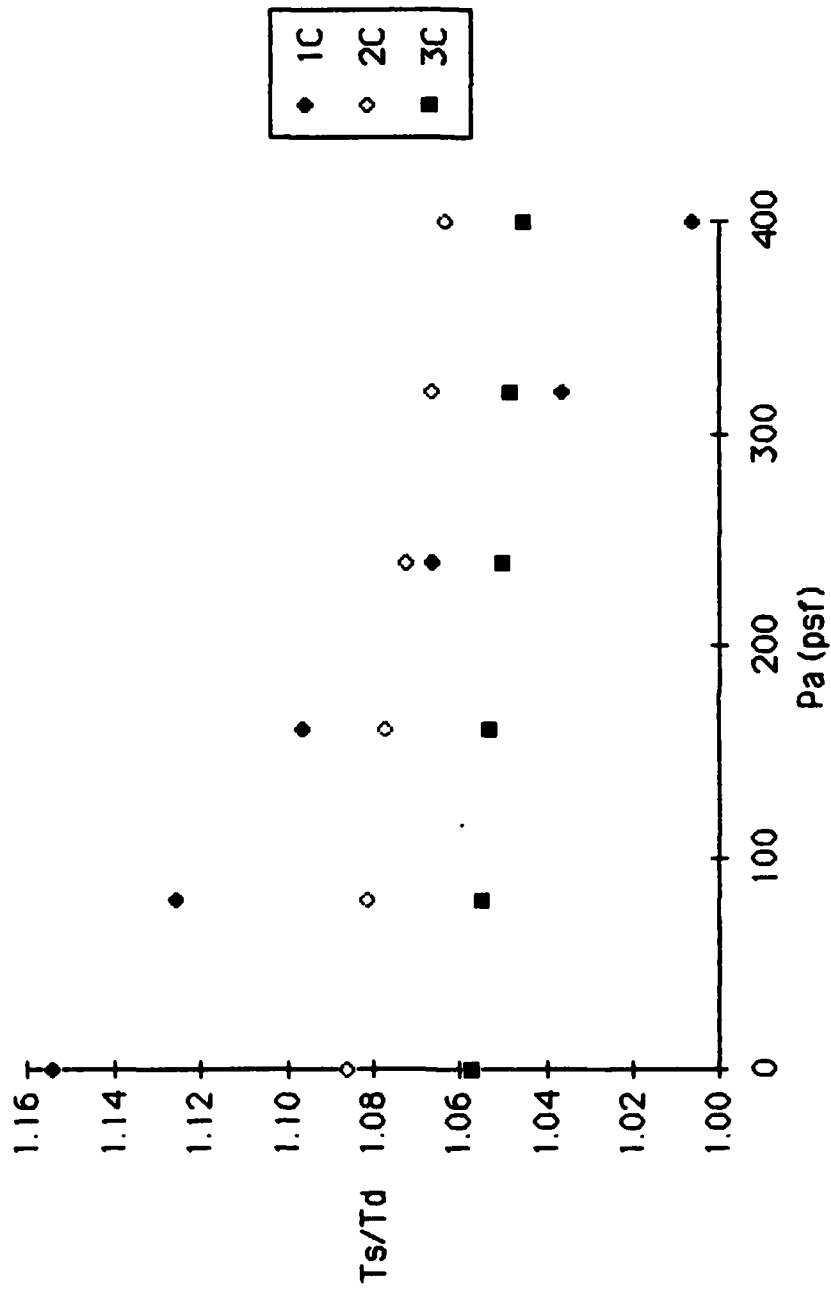


FIGURE 14. NOZZLE C THRUST RATIO

However the configurations with one nozzle were capable of a higher initial thrust ratio. The highest thrust ratio was obtained by the nozzle design with the smallest nozzle area ratio. Nozzle Block C (1:3) had a T_s/T_d of 1.155 and this ratio decreased to 1.08 for Nozzle Block A (1:8) which had the highest area ratio. Those results were based on theoretical performance without losses and further study should be accomplished to establish the flow mechanisms in the mixing region and how they relate to overall performance.

Two-Dimensional Nozzles

In configurations 1A and 1B operating at high pressure ratio (P_c/P_a), all of the exit plane transducers were isolated from the backpressure by the expanding jets interacting with each other and with the shroud. The pressure readings of the transducers remained virtually constant during the test run until the back pressure was sufficient to break the flow attachment to the shroud and eventually the interaction between jets (Figure B-2). Bjurstrom (1) noted a non-uniform base pressure distribution at the exit plane of the nozzle assembly, depending on the configuration and the effective altitude for the test. The relatively uniform base pressure distribution observed in the two-dimensional multi-nozzle assemblies in this investigation (example; Figure A-5) could be the result of the spacing between nozzles. The spacing between the individual nozzle exits for configurations A and B of this investigation were 0.1 and 0.15 inches, respectively. The smallest distance between nozzles of Bjurstrom's (1) nozzles were 0.2 inches and the largest was 1.6

inches. The relatively small distances in this study could have prevented the recirculation patterns noted by Bjurstrom. The schlieren photographs of this study also lacked any visible evidence of the recirculation found in the schlieren photographs of Bjurstrom. Without the recirculation, the trapped area would not have had the additional flow to increase the pressure. This study had three nozzles in a shroud height of two inches as opposed to two nozzles in a corresponding height of four inches. These geometric effects need more study.

In configurations 2A and 2B the replacement of the long shroud with the short shroud increased the pressure ratio at which the flow detached from the shroud. In nozzle block A this pressure ratio increased from PR=20 to PR=23 and in nozzle block B the pressure increase was from PR=15 to PR=17. When the flow separated from the shroud, the P_1 and P_4 transducers experienced a step rise in pressure. This corresponded to a sudden rise to the local backpressure. Upon detachment from the shroud walls, the flow streams remained attached to each other and this flow was inclined toward one of the shroud walls (Figure A-6c). Under this condition, the base pressure on that side remained lower than that on the opposite side (Figure A-5). The inside transducers, P_2 and P_3 , of both nozzle blocks also demonstrated the pressure rise when the pressure ratio (P_c/P_a) was PR=20 for nozzle block A and PR=15 for nozzle block B (Figure A-5, B-3) indicating that the flow from the nozzles had detached from each other.

The relationship between 3B and 4B was similar to that between 1B and 2B with regard to the effect of the shroud length. The longer length

shroud decreased the pressure ratio at which the expanding flow detached from the shroud. In the short shroud configuration of 3B, the pressure ratio was PR=74. While in long shroud configuration of 4B, the pressure ratio at transition decreased to PR=39.

An additional nozzle block was constructed using the 1:4 nozzle area ratio pattern to examine the effect of base injection on flow attachment to the shroud walls. This investigation resulted from configuration 3A, in which a leak on the top of the nozzle block forced the flow away from the shroud. The schlieren photographs in Figure A-8a show this flow characteristic. The new nozzle block was configured similar to 3A to have only a center nozzle in operation, however, the transducers at location P_1 and P_4 were replaced by a fitting connected to a regulated air supply. It was discovered that air injection at both locations would prevent the nozzle flow from attaching to either side of the shroud. In addition, an injection in only one of the locations would cause the jet to attach to opposite side. This is similar to thrust vector control done by Olsen (7) but it uses an injection at the base exit plane rather than injection at the throat of the nozzle. The overall effect of the injection in this case may serve to provide stability to the nozzle flow in the transition from the underexpanded to the overexpanded regime. Additional work in this area is needed to study the control characteristics of base plate injection.

Three-Dimensional Nozzles

Earlier work by Goethert (2) with unshrouded three-dimensional nozzles operating in the underexpanded regime determined that in an

assembly of four nozzles the flow at the center of the nozzle assembly reverses its direction and flows toward the base plate. This recirculation increased the base plate pressure as the flow was turned and exhausted radially through the sides of the nozzle base. Goethert was able to achieve chamber to ambient pressure ratios of 1000, 2.5 times the capability of the AFIT system. With this high chamber to ambient pressure ratio the reverse flow was choked at the minimum area for radial outflow between the nozzles. Under these conditions there is a substantial increase in the central region base pressure. In this study the recirculation noted by Goethert was not detected.

In the three-dimensional shrouded nozzles of this investigation the base region pressure distribution was uniform. This was the result of the flow from the nozzle cluster expanding to the shroud and closing off the base region and the inability of the flow from the individual nozzles to divide the base plate into separate areas of differing pressure. As shown by Figures C-1 to C-3, the base pressure remained relatively constant throughout the test run until the flow detached from the shroud walls. The length of the test run and pressure ratio at transition were dependent upon the number of nozzles in the cluster.

VI CONCLUSIONS

Pressure and flow relationships of three nozzle blocks were studied over a range of test conditions. The apparatus and associated instrumentation were satisfactory for the purpose of this investigation. Results of these lead to the following conclusions:

1. The exhausts of neighboring nozzles interact with each other and the shroud at high pressure ratios. This interaction generates markedly different pressure in the assembly base region than observed with no interaction.

2. The length of the shroud affects the transition of the nozzle with respect to the overall pressure ratio (P_c/P_a) of detachment of the flow from the shroud. The longer shroud permitted operation at a lower pressure ratio without flow detachment from the shroud.

3. The three-dimensional nozzle jets show a marked difference in their interaction when compared to the two-dimensional nozzles. For the two-dimensional models the flow from the individual nozzles, by expanding to the shroud, enclosed the base region into separate areas. These separate areas occurred between each nozzle and between the nozzles and the shroud. The expansion of the flow in the three-dimensional nozzle assembly as expected did not divide the base plate into separate areas of differing pressures. However, the flow from single and multiple three-dimensional nozzles at high PR expanded to the shroud enclosing the entire base region thereby isolating this region from the surrounding ambient conditions.

4. The potential for thrust augmentation is heavily geometry

dependent. With the proper spacing, performance may be affected both through the gas dynamics of the flow, and through the appearance of additional pressure area terms in the base plate region.

VII RECOMMENDATIONS

The following recommendations are suggested for continuation of this work on clustered nozzles:

1. Different nozzle blocks should be tested to examine the effects of the spacing between the individual nozzles, and the spacing between the nozzles and the shroud on the pressure measurements. This would yield information on the effects of any recirculation of the flow in the base region.

2. A means of measuring thrust should be developed to enhance future studies. This measuring device should be designed to have a minimum effect on the flow pattern.

3. Investigate the application of base plate injection as a means of stabilizing the flow for shrouded nozzle assemblies during and after transition that occurs when flow detaches from the shroud. The objective would be to determine the possible applications of base plate injection to thrust vector control.

Bibliography

1. Bjurstrom, D. R. "An Experimental Study of Clustered, Two-Dimensional Rocket Nozzles". M.S. Thesis, Wright-Patterson A.F.B., Ohio: Air Force Institute of Technology, December 1984.
2. Goethert, B. H. Studies of the Flow Characteristics and Performance of Multi-Nozzle Rocket Exhausts. AEDC-TR-59-16. Arnold AFS, Tennessee: ARO, Inc., October 1959. (A.D. 313-155)
3. Hibson, D. H. "Performance Characteristics of Clustered Nozzles". M.S. Thesis, Wright-Patterson A.F.B., Ohio: Air Force Institute of Technology, December 1981.
4. Hill, P. G. and Peterson, C. R. Mechanics and Thermodynamics of Propulsion. Reading, Massachusetts: Addison-Wesley, 1970.
5. Keenan, J. and Kaye, J. Gas Tables. New York: John Wiley and Sons, Inc. 1948.
6. Lester, J. T. "An Experimental Study of Clustered Nozzle Performance". M.S. Thesis, Wright-Patterson A.F.B., Ohio: Air Force Institute of Technology, December 1982.
7. Olsen, R. E. "An Experimental Investigation of a Three-Dimensional Coanda Nozzle". M.S. Thesis, Wright-Patterson A.F.B., Ohio: Air Force Institute of Technology, December 1968.
8. Sutton, G. P. Rocket Propulsion Elements. New York: John Wiley and Sons, Inc., 1964.

Appendix A

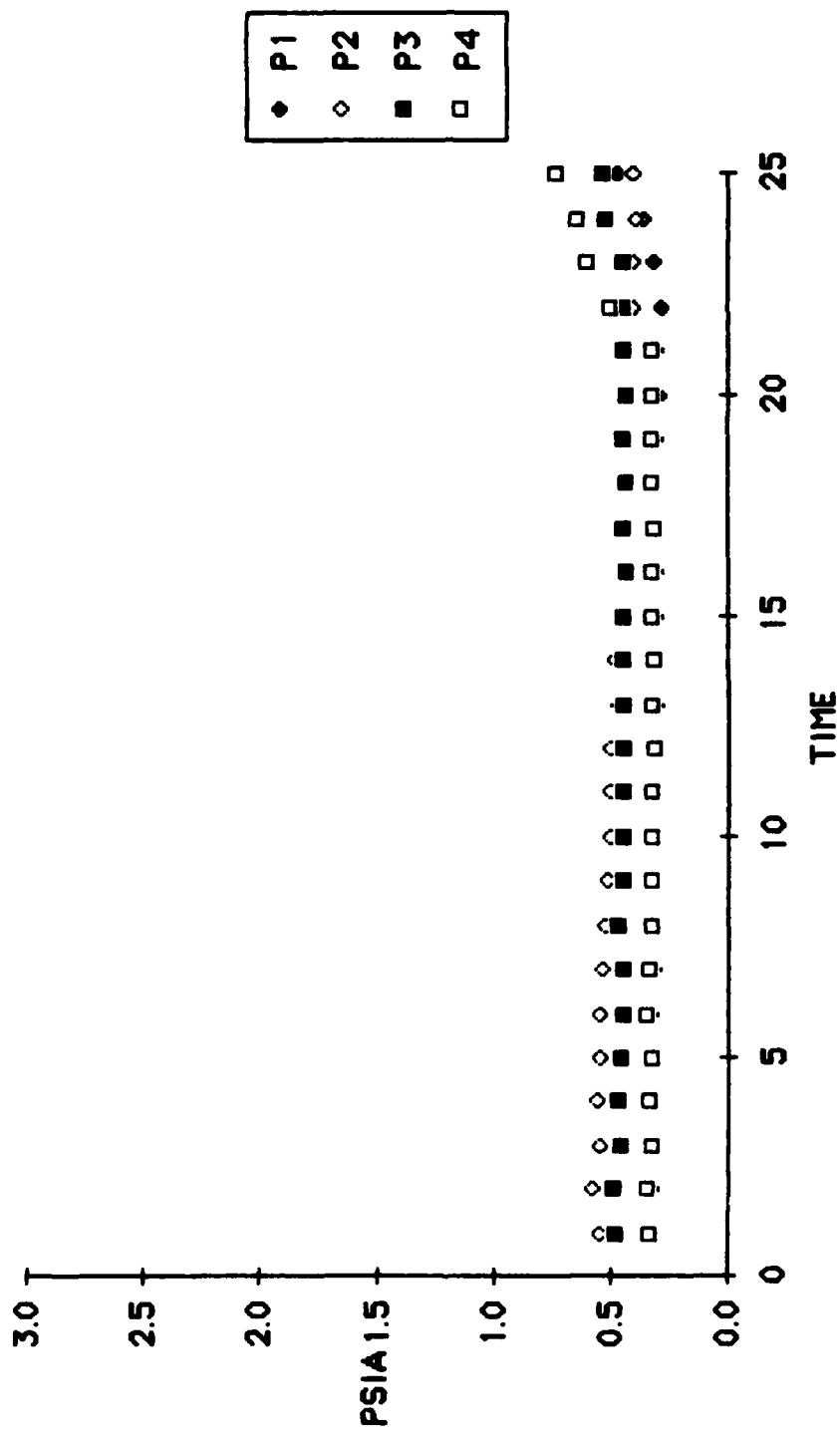


FIGURE A-1. PRESSURE VS TIME FOR CONFIGURATION 1A

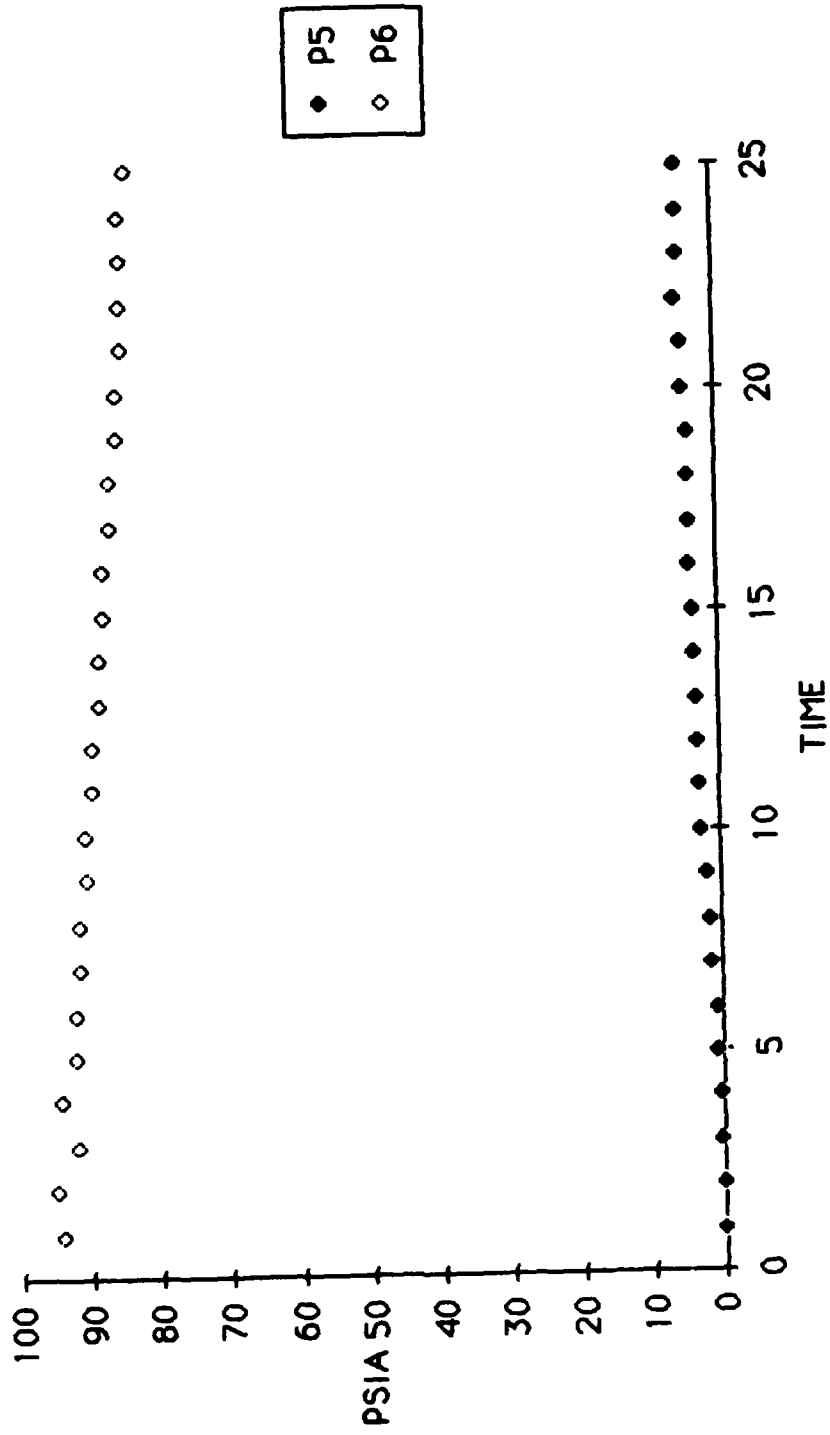


FIGURE A-2. SUPPLY AND BACKPRESSURE FOR 1A

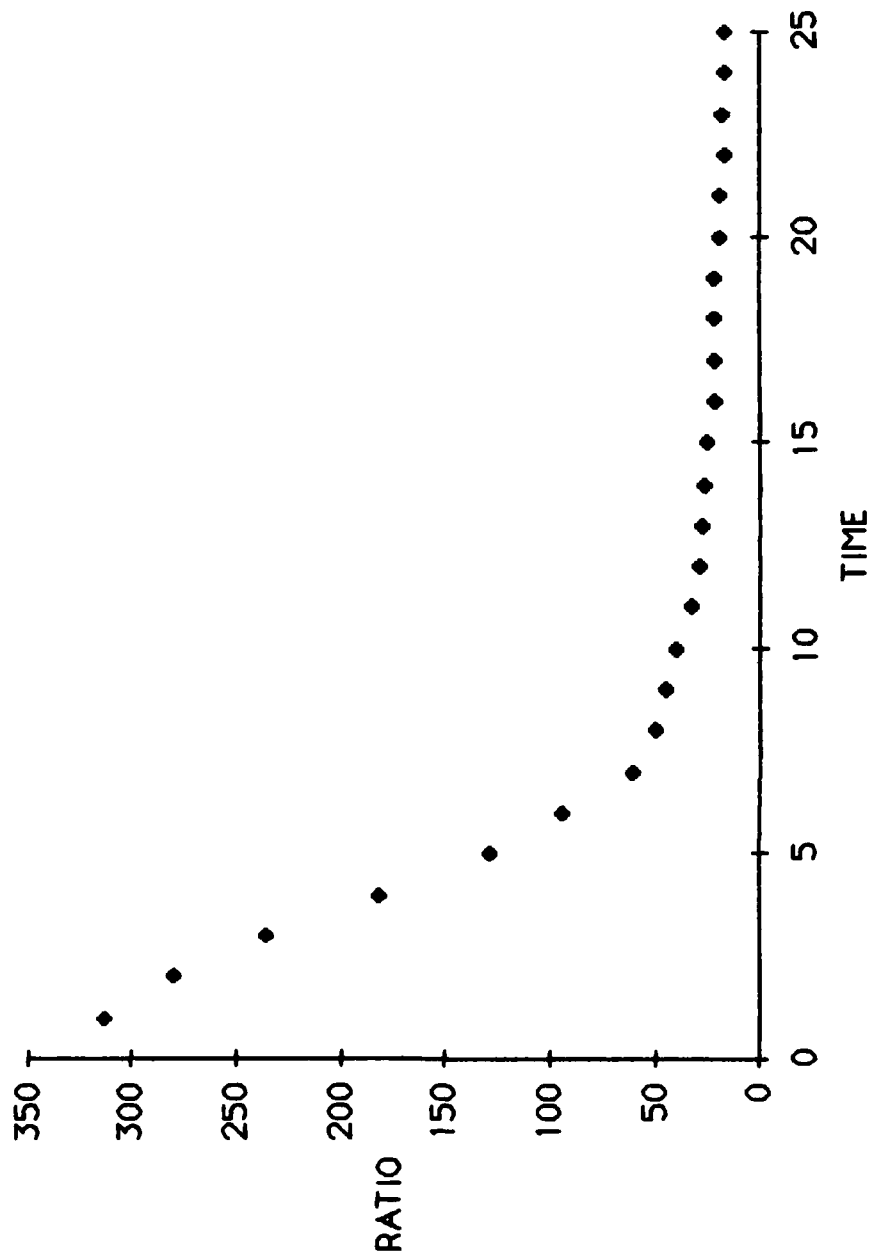


FIGURE A-3. PRESSURE RATIO VS TIME FOR 1A

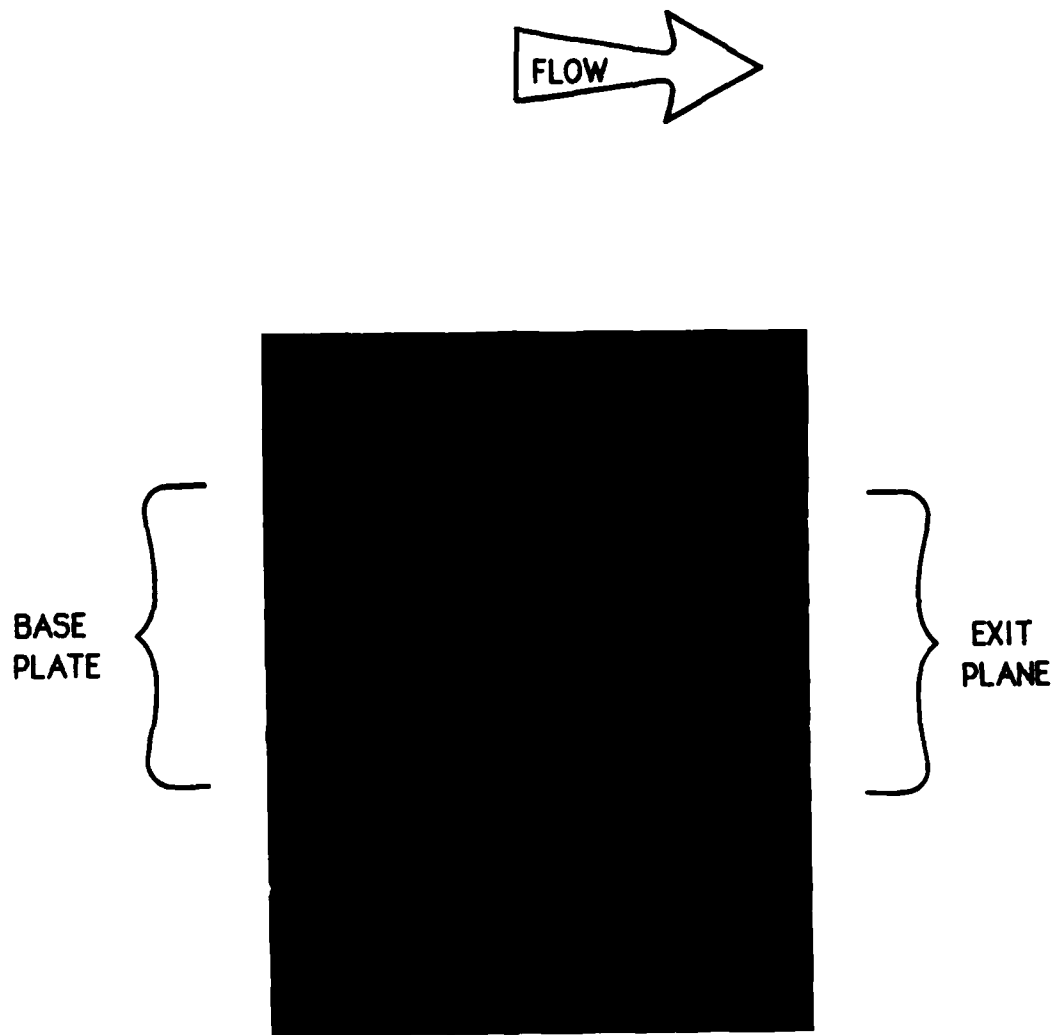


FIGURE A-4. INITIAL CONDITIONS FOR CONFIGURATION 1A

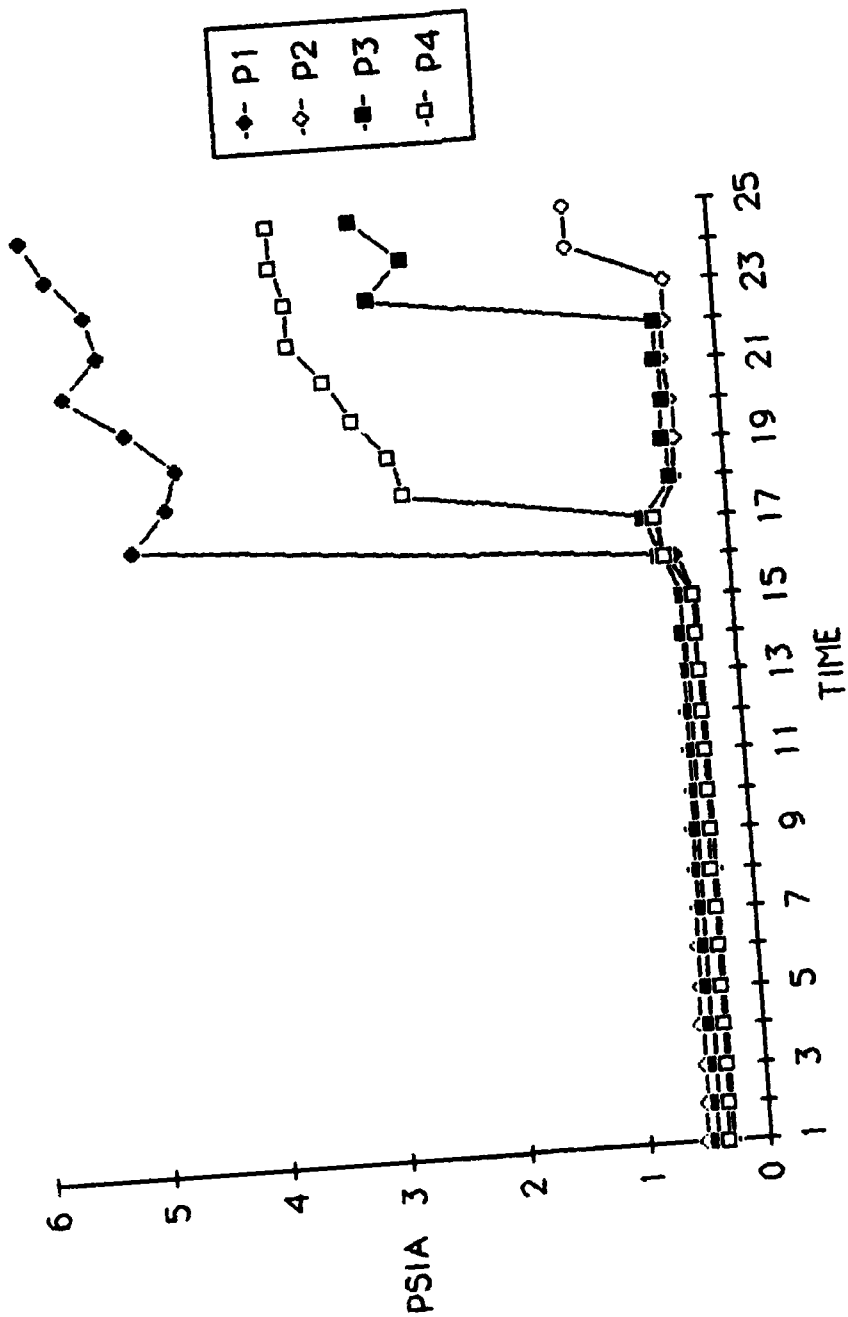


FIGURE A-5. PRESSURE VS TIME FOR CONFIGURATION 2A



a. INITIAL CONDITIONS



b. Pa INCREASING



c. TIME=18-21 SECONDS

FIGURE A-6. SCHLIEREN SERIES FOR CONFIGURATION 2A

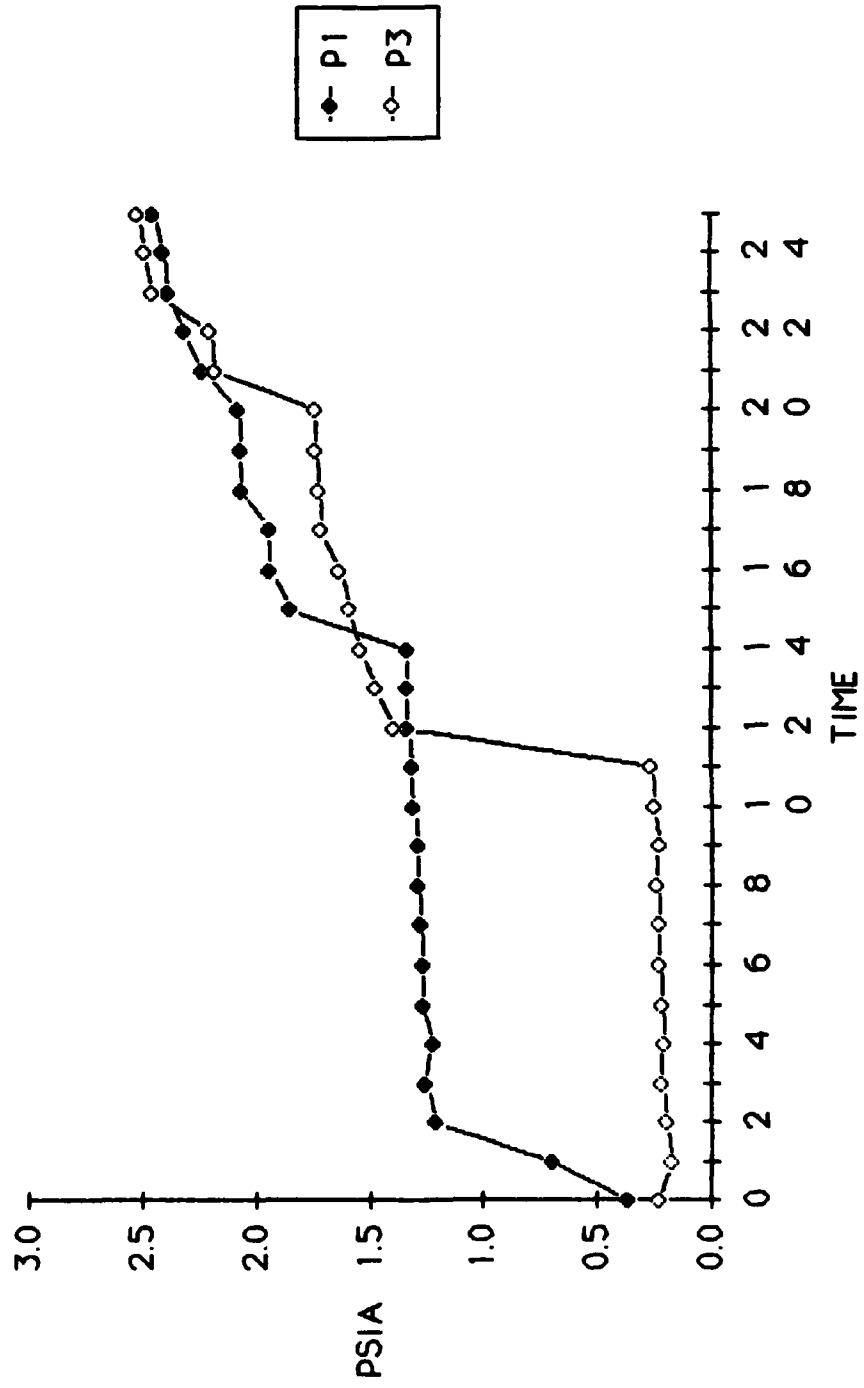


FIGURE A-7. PRESSURE VS TIME FOR CONFIGURATION 3A



a. INITIAL CONDITIONS



b. TIME=12-25

FIGURE A-8. SCHLIEREN SERIES FOR CONFIGURATION 3A

Appendix B

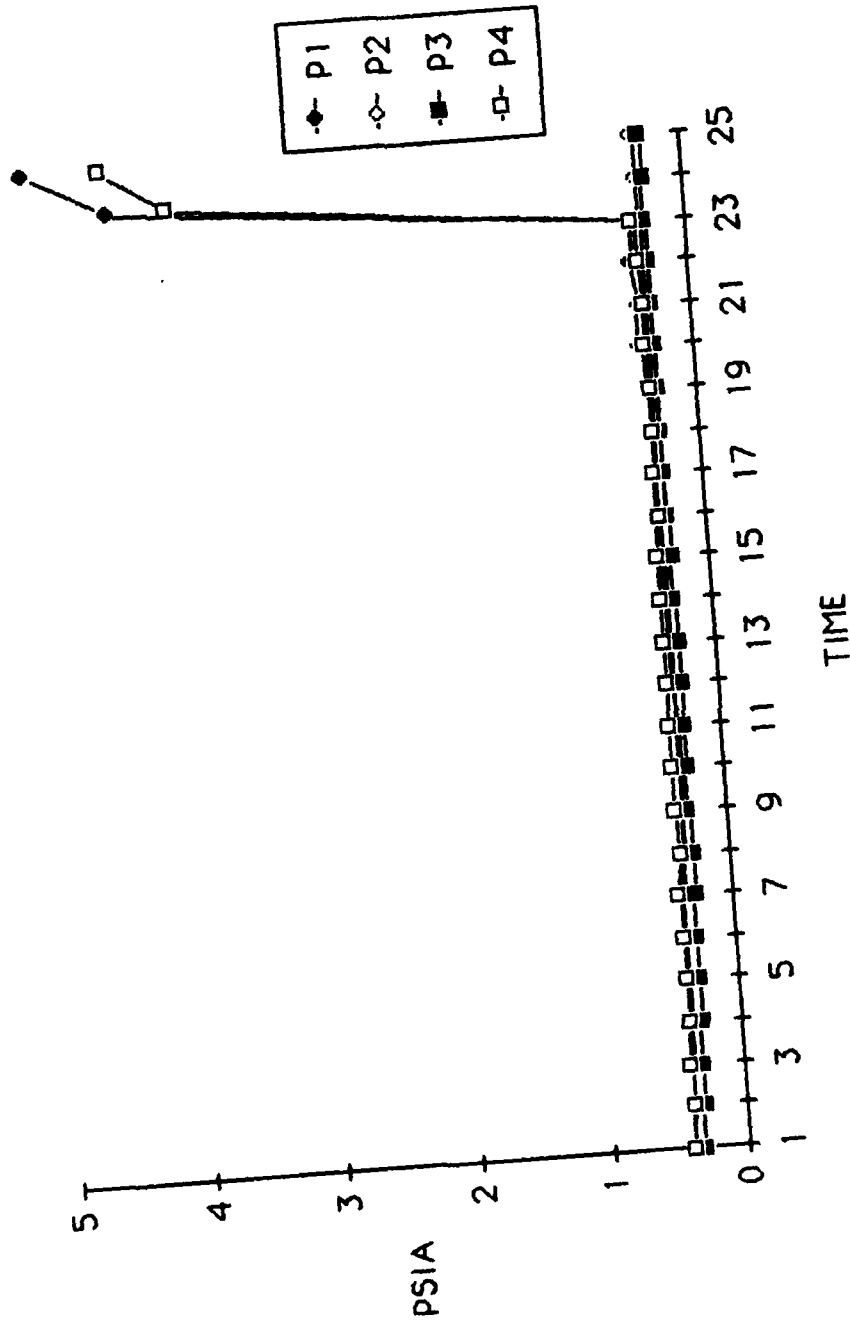


FIGURE B-1. PRESSURE VS TIME FOR CONFIGURATION 1B



FIGURE B-2. INITIAL CONDITIONS FOR CONFIGURATION 1B

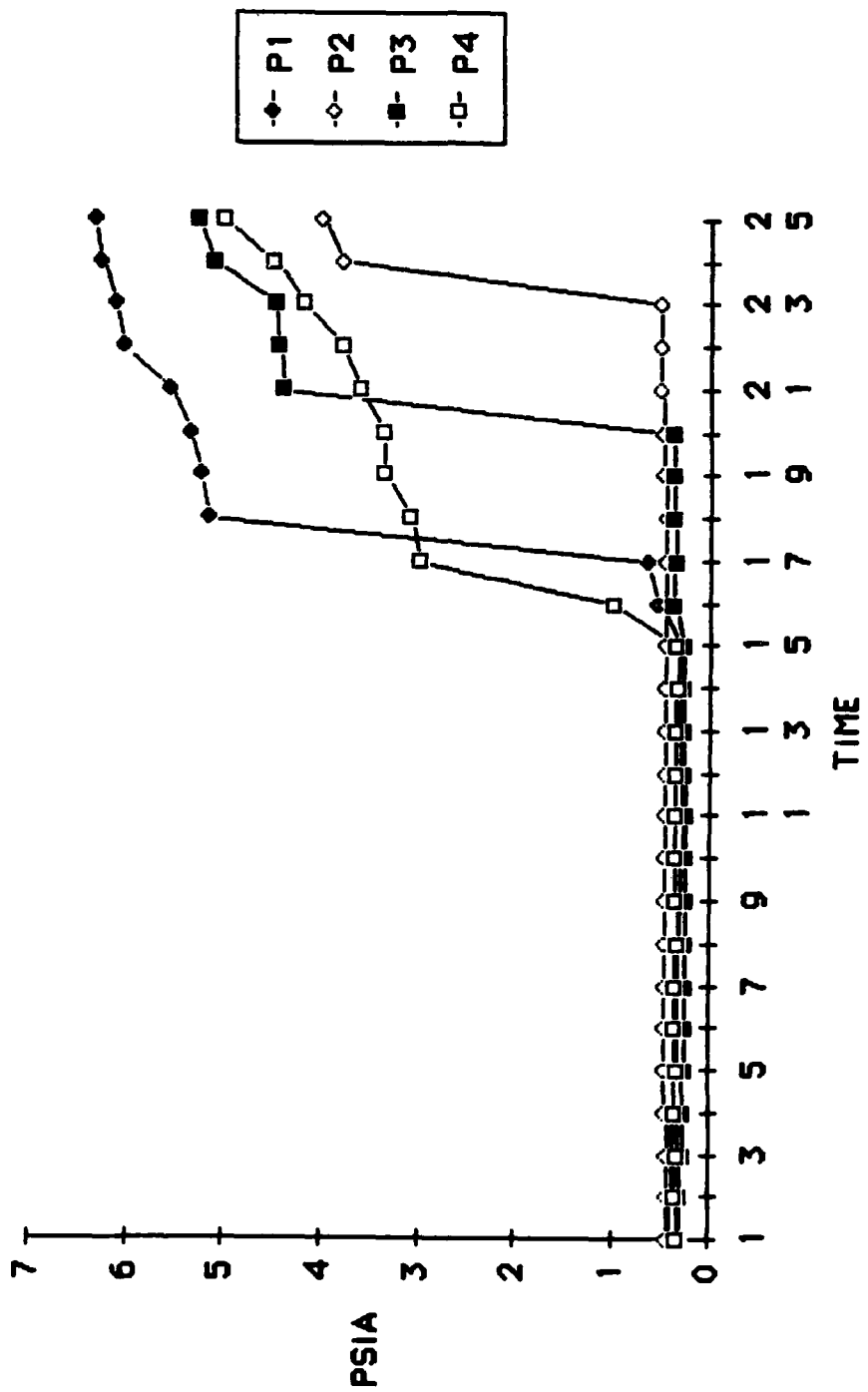


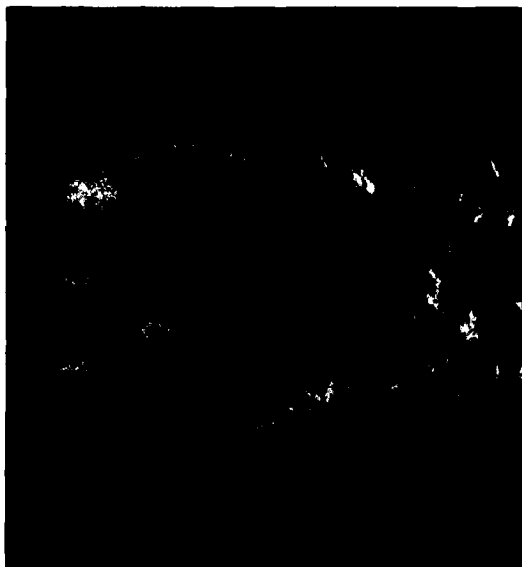
FIGURE B-3. PRESSURE VS TIME FOR CONFIGURATION 2B



a.



b.



c.



d.

FIGURE B-4. SCHLIEREN SERIES FOR CONFIGURATION 2B

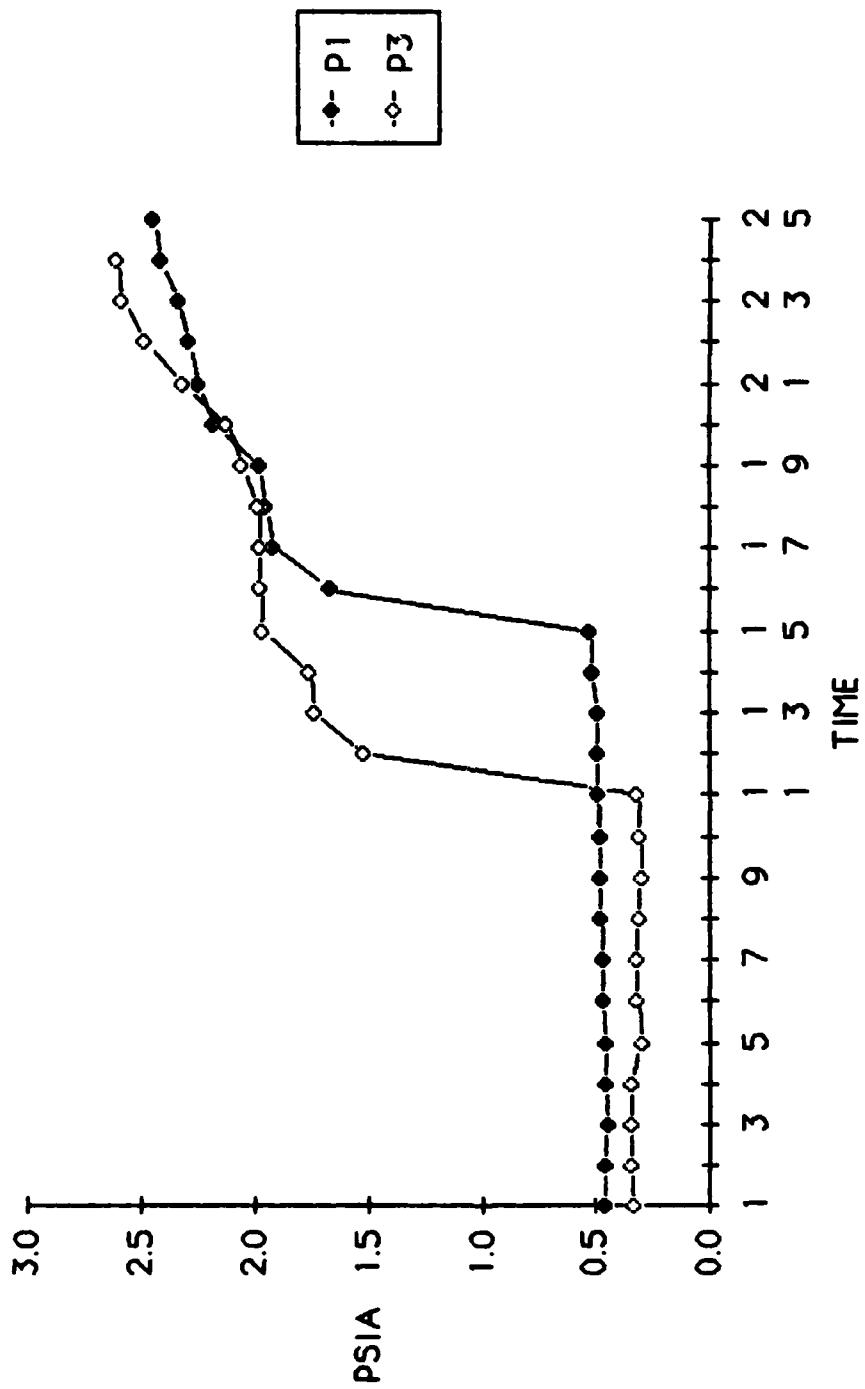
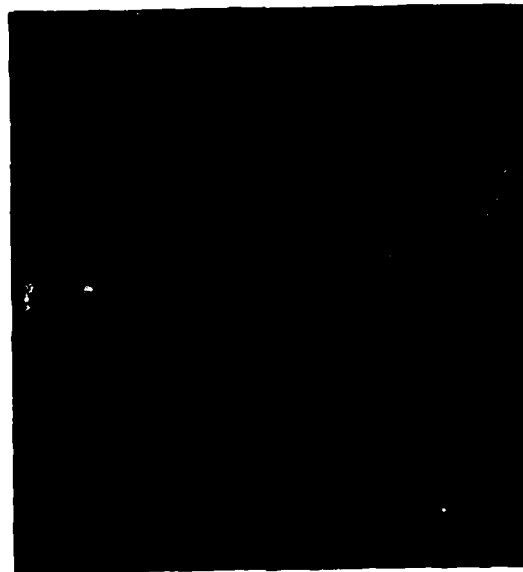


FIGURE B-5. PRESSURE VS TIME FOR CONFIGURATION 3B



a. INITIAL CONDITIONS



b. FLOW DETACHMENT FROM SHROUD

FIGURE B-6. SCHLIEREN SERIES FOR CONFIGURATION 3B

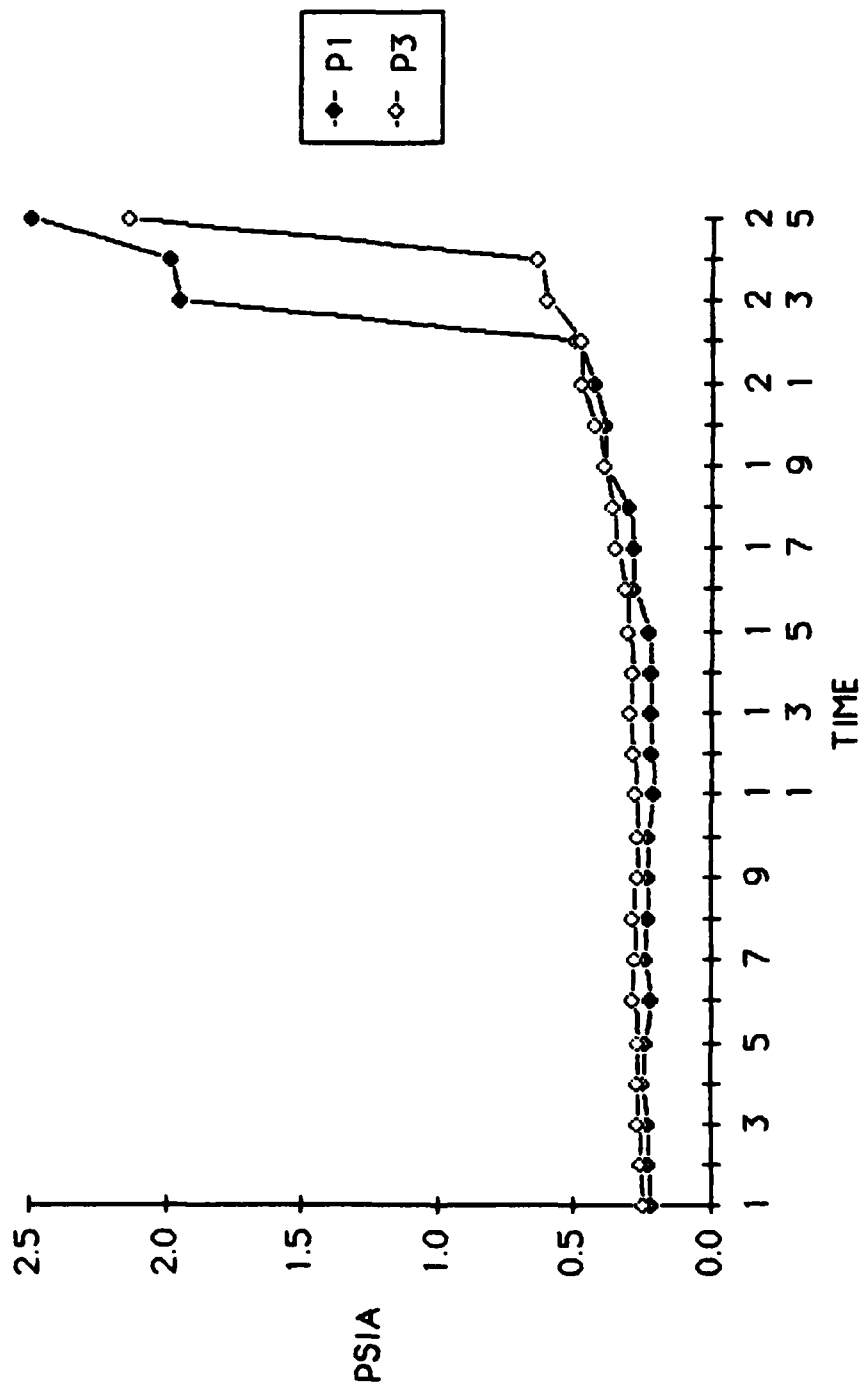


FIGURE B-7. PRESSURE VS TIME FOR CONFIGURATION 4B



FIGURE B-8. INITIAL CONDITIONS FOR CONFIGURATION 4B

Appendix C

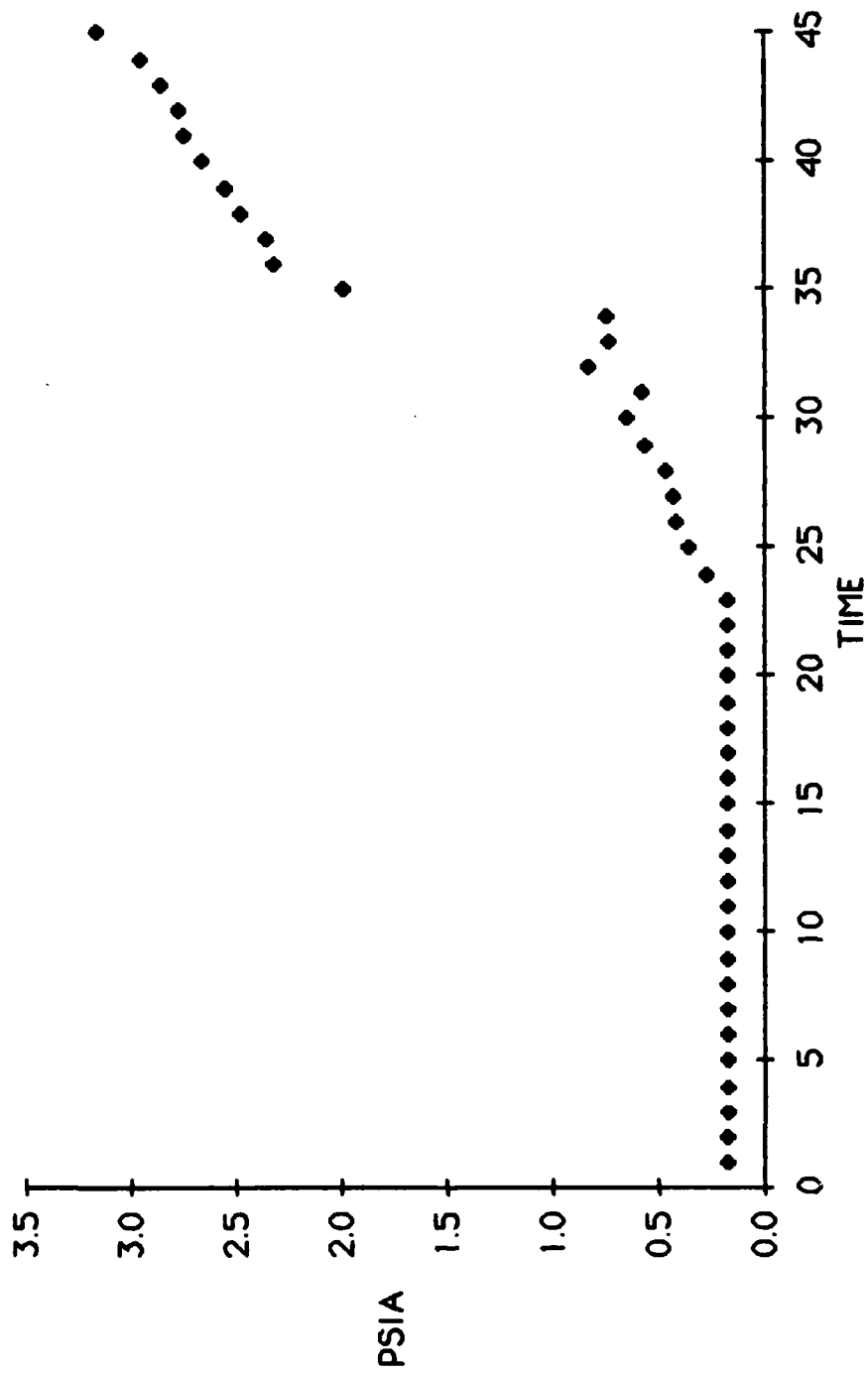


FIGURE C-1. PRESSURE VS TIME FOR CONFIGURATION 1C

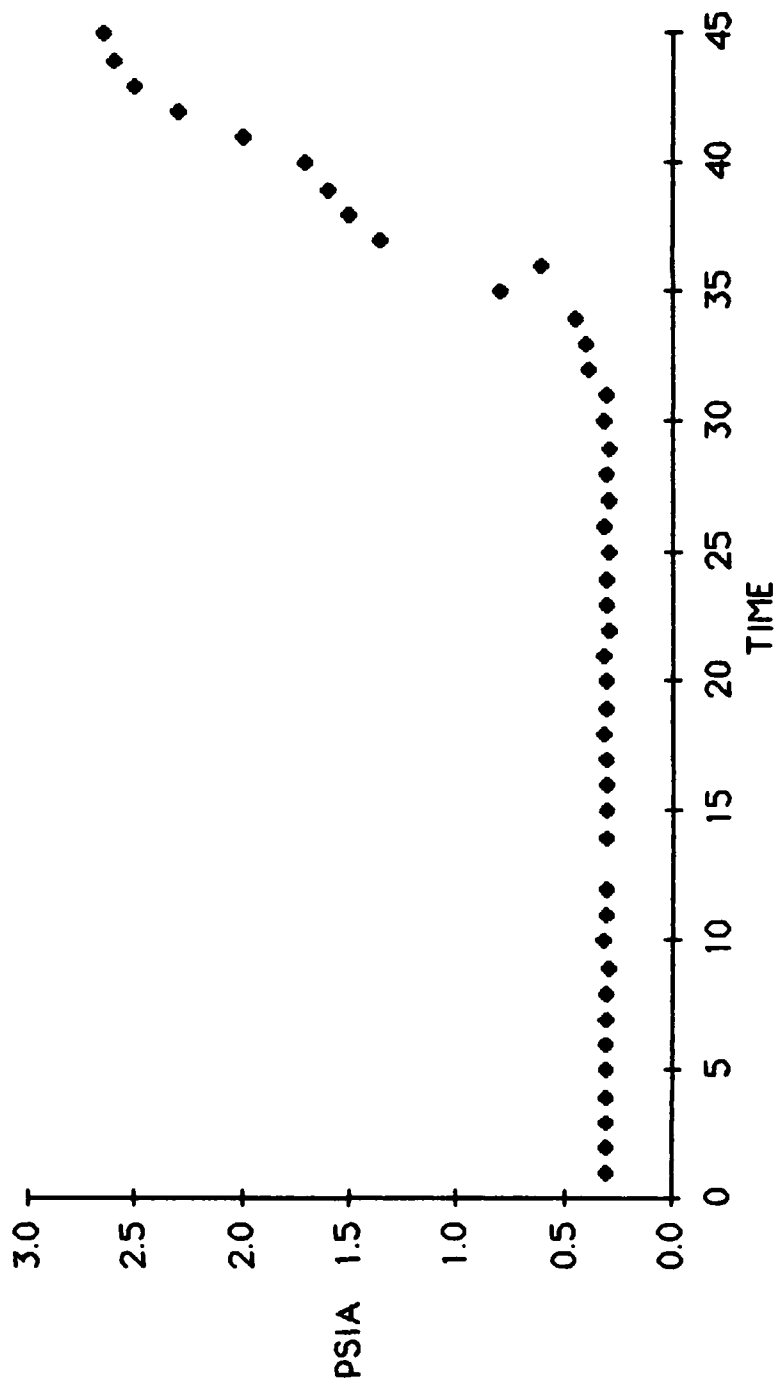


FIGURE C-2. PRESSURE VS TIME FOR CONFIGURATION 2C

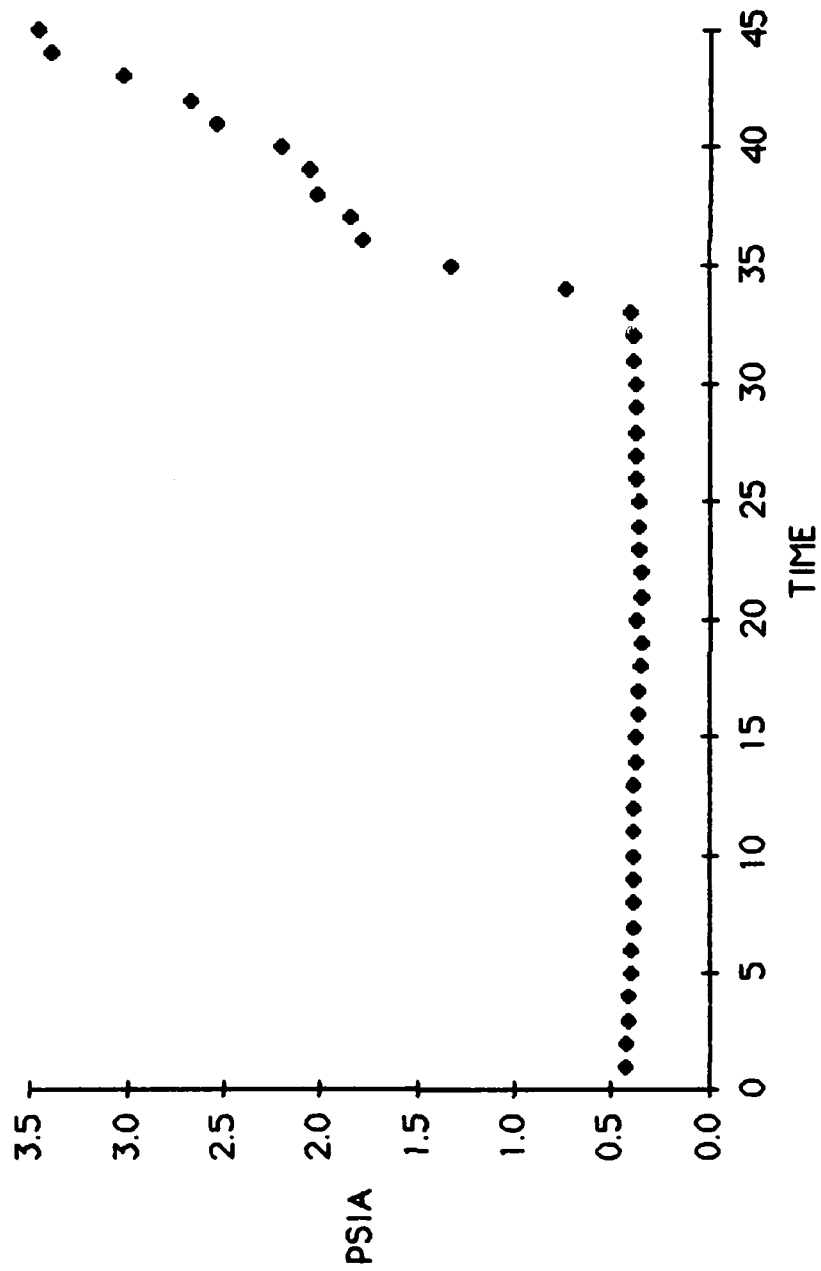


FIGURE C-3. PRESSURE VS TIME FOR CONFIGURATION 3C

Vita

Captain James R. Moran was born on 13 January 1957 in Hopewell, Virginia. In June 1979, he received his BS degree in Engineering and Applied Science from the United States Military Academy, West Point, New York. Upon graduation he was awarded an RA commission as a 2Lt in the US Army Ordnance Corps. Captain Moran has served in a variety of assignments to include, Platoon Leader, Shop Officer and Company Commander of a Heavy Division Forward Support Maintenance Company. Captain Moran entered the Air Force Institute of Technology in May, 1984.

Permanent address: Lockport, New York

REPORT DOCUMENTATION PAGE

1. REPORT SECURITY CLASSIFICATION UNCLASSIFIED		1b. RESTRICTIVE MARKINGS			
2a. SECURITY CLASSIFICATION AUTHORITY		3. DISTRIBUTION/AVAILABILITY OF REPORT Approved for public release; distribution unlimited.			
2b. DECLASSIFICATION/DOWNGRADING SCHEDULE					
4. PERFORMING ORGANIZATION REPORT NUMBER(S) AFIT/GAE/AA/85D-11		5. MONITORING ORGANIZATION REPORT NUMBER(S)			
6a. NAME OF PERFORMING ORGANIZATION School of Engineering	6b. OFFICE SYMBOL <i>(If applicable)</i> AFIT/ENG	7a. NAME OF MONITORING ORGANIZATION			
6c. ADDRESS (City, State and ZIP Code) Air Force Institute of Technology Wright-patterson AFB, Ohio 45433		7b. ADDRESS (City, State and ZIP Code)			
8a. NAME OF FUNDING/SPONSORING ORGANIZATION	8b. OFFICE SYMBOL <i>(If applicable)</i>	9. PROCUREMENT INSTRUMENT IDENTIFICATION NUMBER			
8c. ADDRESS (City, State and ZIP Code)		10. SOURCE OF FUNDING NOS.			
11. TITLE (Include Security Classification) See Box 19		PROGRAM ELEMENT NO.	PROJECT NO.	TASK NO.	WORK UNIT NO.
		12. PERSONAL AUTHOR(S) James R. Moran, CPT OrdC, USA			
13a. TYPE OF REPORT MS Thesis	13b. TIME COVERED FROM _____ TO _____	14. DATE OF REPORT (Yr., Mo., Day) 1985 December	15. PAGE COUNT 81		
16. SUPPLEMENTARY NOTATION					
17. COSATI CODES			18. SUBJECT TERMS (Continue on reverse if necessary and identify by block number)		
FIELD	GROUP	SUB. GR.	Clustered Nozzles, Shroud, Three-Dimensional Two-Dimensional		
01	03				
19. ABSTRACT (Continue on reverse if necessary and identify by block number)					
Title: An Experimental Study of Clustered Nozzles with Variable Shroud			Approved for public release: LAW AFR 180-1. <i>Fern Wolaver</i> LYNN E. WOLAVER 12 JAN 86 Dean for Research and Professional Development Air Force Institute of Technology (AFIT) Wright-Patterson AFB OH 45433		
Thesis Advisor: William C. Elrod Department of Aeronautics and Astronautics					
20. DISTRIBUTION/AVAILABILITY OF ABSTRACT UNCLASSIFIED/UNLIMITED <input checked="" type="checkbox"/> SAME AS RPT. <input type="checkbox"/> DTIC USERS <input type="checkbox"/>			21. ABSTRACT SECURITY CLASSIFICATION UNCLASSIFIED		
22a. NAME OF RESPONSIBLE INDIVIDUAL William C. Elrod, Professor		22b. TELEPHONE NUMBER <i>(Include Area Code)</i> 513-255-2562	22c. OFFICE SYMBOL AFIT/ENY		

The *of this thesis*
→ This research involved the investigation of pressure and flow fields in the base region of clustered nozzles during cold flow testing. Nozzle exit conditions simulating altitudes up to 75,000 feet and chamber-to-back pressure ratios up to 200 were used. The nozzle clusters considered were made up of sets of two and three dimensional supersonic convergent-divergent nozzles with a square shroud around the cluster. The two dimensional nozzles had design exit Mach numbers of 3.68 and 2.94. The three dimensional nozzles had a design exit Mach number of 2.64. The nozzle clusters were studied using various configurations and with two shroud lengths. A schlieren system that allowed for both still photographs and motion picture film was used to investigate the flow fields.

The results of this study indicate that the pressure fields in the base region of a nozzle cluster are dependent on both geometry and on the operating altitude. The outer wall of the test section (shroud) adjacent to the nozzles was observed to significantly affect the flow patterns and measured pressures. Potential influences in performance exist due both to changes in the gas dynamics of the flow and the appearance of additional pressure-area forces.

END

FILMED

3 - 86

DTIC